University of Hertfordshire UH

School of Engineering and Computer Science

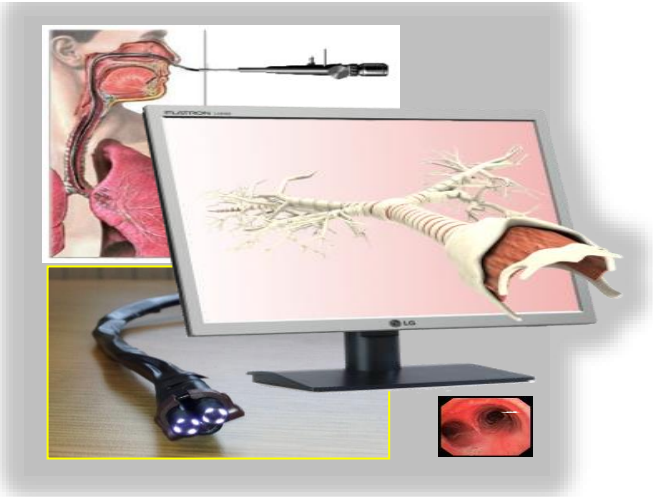

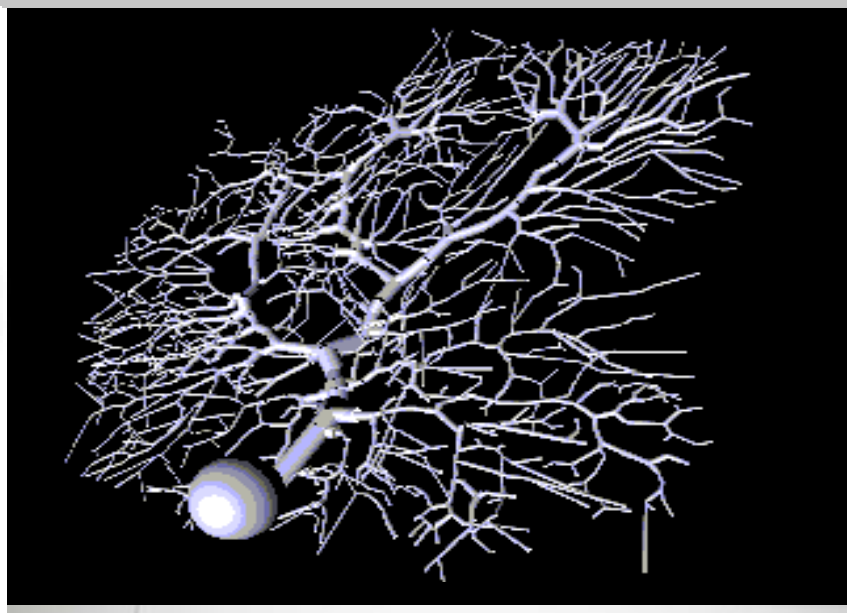

PROCEEDINGS OF ABSTRACTS ENGINEERING AND COMPUTER SCIENCE RESEARCH CONFERENCE 2019

Wednesday 17 April 2019

University of Hertfordshire, Hatfield, UK

Editor: Loïc Coudron

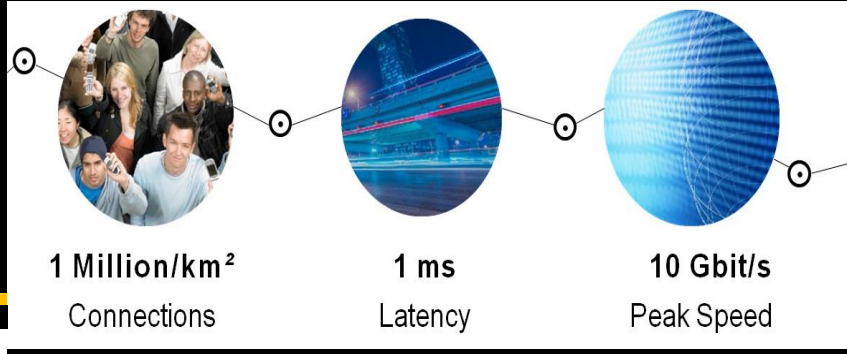

University of Hertfordshire UH

School of Engineering and Computer Science

Proceedings of Abstracts Engineering and Computer Science Research Conference, 17th April 2019, University of Hertfordshire, Hatfield, UK

Editor Loïc Coudron

Published online: UH Research Archive, September 2019

Published by
University of Hertfordshire
College Lane
Hatfield
AL10 9AB
United Kingdom

DOI: 10.18745/pb.21692

URL: https://doi.org/10.18745/pb.21692

Contact
Dr Loic Coudron
Centre for Biodetection Technologies,
Centre for Engineering Research,
Microfluidics and Microengineering Research Group.

School of Engineering and Technology
University of Hertfordshire
College Lane, Hatfield, Herts, AL10 9AB, UK
Email: l.coudron@herts.ac.uk
Tel: +44 (0)1707 286174

Preface

Dear reader of these proceedings,

Welcome to our record of abstracts submitted and accepted for presentation at the Inaugural Engineering and Computer Science Research Conference held 17th April 2019 at the University of Hertfordshire, Hatfield, UK.

This conference is a local event aiming at bringing together the research students, staff and eminent external guests to celebrate Engineering and Computer Science Research at the University of Hertfordshire.

The ECS Research Conference aims to showcase the broad landscape of research taking place in the School of Engineering and Computer Science. The 2019 conference was articulated around three topical cross-disciplinary themes: Make and Preserve the Future; Connect the People and Cities; and Protect and Care.

Following the success of the inaugural edition, the 2nd ECS Research conference will take place the 8th April 2020. The aim is to make this event a long-term yearly acknowledgement of Engineering and Computer Science Research at UH.

Scientific Committee

Prof. Yong Chen Head of the Energy and Sustainable Design Research Group

Prof. Andreas Chrysanthou Head of the Material and Structure Research Group

Dr Ian Johnston Head of the BioEngineering Research Group

Dr Raimund Kirner Head of the Algorithms Research Group

Dr Pandelis Kourtessis Associate Dean (Research), School of Engineering and Computer Science

Dr Daniel McCluskey Associate Dean Enterprise (Engineering), Head of the Microfluidics and Engineering Research Group

Prof. Daniel Polani Head of the Adaptive Systems Research Group

Dr Volker Steuber Associate Dean (Research, CS), Head of the Biocomputation Research Group

Prof. Yichuang Sun Head of the Communications and Intelligent Systems Research Group

Organising Committee

Dr Loïc Coudron, Centre for Biodetection Technologies, Centre for Engineering Research, Microfluidics and Microengineering Research Group.

Dr Christabel Tan, Centre for Biodetection Technologies, Centre for Engineering Research, Microfluidics and Microengineering.

Dr Zoe Jeffrey, Centre for Engineering Research, Communications and Intelligent Systems

Dr Mouloud Denai, Centre for Engineering Research, Communications and Intelligent Systems

Awards

The Best Contributed Talk was awarded to Nathan Counsel for his outstanding Oral Presentation titled "*Development of enhanced power generation for piezoelectric energy harvesting*"

The Best Poster was awarded to Rebecca Miko for her outstanding Poster Presentation titled "*Brain-inspired spiking neural network for gas-based navigation"*

Congratulations to our delegates for their excellent contributions.

Acknowledgement

The members of the organising Committee are grateful to the eminent guests who accepted the invitation to share their inspiring experience with our delegates:

Mr Nikhil Vasdev, Consultant Urological Surgeon / Urology Cancer Pathway Lead, Hertfordshire and Bedfordshire Urological Cancer Centre, Department of Urology, Lister Hospital (East and North Herts NHS Trust), Watford General Hospital (West Herts NHS Trust), who gave us an insight on the future of care and surgery with a lecture on *Robotic Surgery and Engineering - Present and Future developments*

Dr Deborah Pullen*,* Executive Director BRE Trust, who shared her inspiring vision on *The Enhancement of Social Value through Integrated Engineering*

Professor Hom Nath Dhakal, Coordinator, Advanced Materials and Manufacturing (AMM) Research Group, School of Mechanical and Design Engineering, University of Portsmouth, who presented his cutting-edge research on *Hybridisation approach into advanced composites and Biocomposites for improved performance: Mechanisms, opportunities and challenges*

Dr Brian Crook, Science Division Microbiology Team leader, Health and Safety Executive, who guide us through the simulation and validation of new clinical procedure using *Fluorescence visualisation to evaluate effectiveness of personal protective equipment for infection control*

Dr Raimund Kirner and Dr Olga Tveretina, Centre for Computer Science and Informatics Research, School of Engineering and Computer Science, University of Hertfordshire, who gave an in-depth overview of their research in *Interfaces and concepts to build large resilient and predictable systems*

We wish to acknowledge, for their valuable support during the organisation of the event and their contribution to the programme during the conference:

Professor Quintin McKellar, Vice-Chancellor

Professor John Senior, Pro Vice-Chancellor (Research and Enterprise)

Dr Rodney Day, Dean of the School of Engineering and Computer Science

Dr Susan Grey, Director of the Doctoral College

We would like to thank all delegates for their excellent contributions to the conference. Special thanks to Dr Kourtessis, Professor Chen, Dr Johnston, Dr Steuber for chairing the conference sessions. We are grateful to the judging panel for attributing the conference award. Finally, we would like to thank the UH Events Team (Julie Melton, Mercedes Brazier and Frances Elliott) for their tremendous help for organising and running the event.

Table of Contents

Conference Programme

Morning

8:40 – 8:55 registration and Coffee

Plenary session – chaired by Dr Pandelis Kourtessis

8:55 – 9:00 **Dr Loic Coudron**, Organising Committee – *Introduction*

9:00 – 9:10 **Prof. Quintin McKellar**, Vice-Chancellor – *Welcoming speech*

9:10 – 9:50 **Mr Nikhil Vasdev**, Consultant Urological Surgeon / Urology Cancer Pathway Lead, Hertfordshire and Bedfordshire Urological Cancer Centre, Department of Urology, Lister Hospital (East and North Herts NHS Trust), Watford General Hospital (West Herts NHS Trust) – *Robotic Surgery and Engineering - Present and Future developments*

9:50 – 10:30 **Dr Deborah Pullen***,* Executive Director BRE Trust - *The Enhancement of Social Value through Integrated Engineering.*

Coffee Break

10:30 – 10:50 Coffee Break

Session 1 – Make and preserve the future – chaired by Professor Yong Chen

10:50 – 11:20 **Keynote speech: Professor Hom Nath Dhakal**, Coordinator, Advanced Materials and Manufacturing (AMM) Research Group, School of Mechanical and Design Engineering, University of Portsmouth – *Hybridisation approach into advanced composites and Biocomposites for improved performance: Mechanisms, opportunities and challenges*

11:20 – 11:35 **Nathan Counsel** – *Development of enhanced power generation for piezoelectric energy harvesting*

11:35 – 11:50 **Richard Nwawe** – *Optimisation of a gigacycle fatigue biaxial specimen for ultrasonic testing*

11:50 – 12:05 **Helen Partou** – *A Gamified Prototype for Software Requirements Engineering*

Lunch and Poster session

12:05 - 13:30 Lunch and Poster session

List of posters:

Brain-inspired spiking neural network for gas-based navigation - **Rebecca Miko**

A scale-up of processing and LCA comparison of non-woven flax tape and triaxial glass fibre reinforced composites - **Gilles Toffe**

Investigating the effects of tooling materials, drill geometry and process parameters on hole quality of flax FRP composite laminate - **Dr Sikiru Oluwarotimi Ismail**

Using feature weighting as a tool for clustering applications - **Deepak Panday**

Modal parameters response to increased energy absorption in CFRP laminates - **Daerefa-a Mitsheal Amafabia**

Improving energy disaggregation performance using appliance-driven frame-lengths - **Pascal A. Schirmer**

Measuring Habituation during Human-Robot Interaction - **Grigorios D. Skaltsas**

Politics and Power in Software Requirements Engineering - **Rana Siadati**

Searching for Asynchronous Irregular Activity in Balanced Real Time Spiking Neural Networks: Reproducing a Parameter Search using Neuromorphic Hardware - **Samuel Sutton**

Graphene Aerogel deposition methods and its fabrication techniques as Energy storage devices - **Himayasri Rao Lekkala**

Modelling Adaptation through Social Allostasis: Modulating the Effects of Social Touch with Oxytocin in Embodied Agents - **Imran Khan**

The role of cerebellar short-term synaptic plasticity in the pathology and medication of downbeat nystagmus - **Julia Goncharenko**

Validation of a DNA library preparation model using a genetic algorithm - **Nathan Beka**

The Correlation between EEG Signals Varying with Distance for Datasets With and Without Medical Condition - **Ronakben Bhavsar**

Computational Dynamics of Complex Biochemical Systems - **Ágnes Bonivárt**

Afternoon

Session 2 – Connect the people and cities – chaired by Dr Ian Johnston

13:30 – 14:00 **Keynote speech: Dr Raimund Kirner and Dr Olga Tveretina**, Centre for Computer Science and Informatics Research, School of Engineering and Computer Science, University of Hertfordshire – *Interfaces and concepts to build large resilient and predictable systems*

14:00 – 14:15 **Alok Verma** – *Data fusion in Internet of Things*

14:15 – 14:30 **Paul Canoville** – *Numerical Methods for the Thermal Design and Analysis of Airframe Structures for High Speed Aerospace Vehicles*

14:30 – 14:45 **Matthew Robinson** – *Software Defined Networking for 5G compatible Enhanced WiFi Video Broadcasting*

Coffee Break

14:45 – 15:05 Coffee Break

Session 3 – Protect and Care – chaired by Dr Volker Steuber

15:05 – 15:35 **Keynote speech: Brian Crook** – Science Division Microbiology Team leader – Health and Safety Executive - *Fluorescence visualisation to evaluate effectiveness of personal protective equipment for infection control*

15:35 – 15:50 **Richard Kaye** – *Development of a fieldable autonomous optical detection system for the detection of waterborne pathogens*

15:50 – 16:05 **Damien Drix** – *Sparse Coding with a Somato-Dendritic Learning Rule*

16:05 - 16:20 **Ankur Sinha** – *Investigating activity dependent dynamics of synaptic structures using biologically plausible models of post-deafferentation network repair*

Closing remarks – Professor John Senior – Prizes – Wine and Cheese

16:20 – 16:30 closing remarks by Professor John Senior, Pro Vice-Chancellor (Research and Enterprise)

16:30 – 17:00 Prizes announcement, wine and cheese degustation

Session 1: Make and preserve the future

Session chaired by Professor Yong Chen

Optimisation of a gigacycle biaxial fatigue specimen for ultrasonic testing

Richard Nwawe[1], Marzio Grasso[2], Yong Chen[3], Jan Klusak[4], Vincenzo Rosiello[5]

[1,3]University of Hertfordshire, UK
[2]University of Kingston, UK
[4]CEITEC Institute of Physics of Materials, Czech Republic
[5]University of Naples Federico II, Italy
*Richard Nwawe: rnwawe@gmail.com

An optimisation process based on the computation of the modal response and biaxial stress state profile of a biaxial specimen is presented with a view to obtain a suitable gigacycle biaxial specimen. The specimen geometries are investigated and optimised around 7 geometry governing parameters and three main optimisation criteria have to be met. From the iterative optimisation process, two satisfactory specimen concepts (spherical and cylindrical) are obtained. The optimal geometrical parameter value ranges, guaranteeing the production of fine-tuned gigacycle biaxial specimens fit for ultrasonic fatigue testing are acquired from an evaluation of each parameter influence on the specimen response.

Keywords: gigacycle fatigue; biaxial stress; geometry optimisation; ultrasonic testing; biaxial fatigue specimen

Introduction

The higher performance requirements for modern engineering structural parts such as cylinder heads or gas turbine disks have stimulated investigations beyond the standard fatigue endurance limit (10^7 cycles) into the gigacycle fatigue range (beyond 10^9 cycles)[1,2]. Investigating the combined effect of a biaxial stress state on material in the gigacycle range would allow a better characterisation of the material in terms of its fatigue characteristics (strength, life, crack nucleation and propagation) under complex loading. The main obstacles for biaxial fatigue research in the gigacycle range are the absence of a suitable specimen similar to the cruciform specimen, capable at lower fatigue ranges to produce a uniform biaxial stress in the material. ; coupled to the inadequacy of testing equipment such as the ultrasonic machine to induce a biaxial stress state in the tested material [3,4]. The limitations observed in literature have demonstrated the need for a standard biaxial specimen to enable a more holistic investigation of gigacycle fatigue. This paper suggests a numerical optimisation method developed to obtain two viable concepts for a biaxial specimen to utilise in ultrasonic testing under a uniaxial excitation.

Methodology

For the investigation presented in this paper, an iterative optimisation process is devised in order to obtain a suitable biaxial gigacycle specimen. The optimisation process relies on the careful identification of 7 geometrical parameters governing the modal response and stress field profile of the biaxial specimen.

The geometry considered for optimisation was suggested in the work of Bellett et al. [5] and optimised with the use of ANSYS APDL macros to obtain the final geometries presented in Figure 1. Three optimisation criteria are observed to obtain the final specimens geometries.

- The tension-tension T⊕T mode shape had to be within the range 20±0.5 kHz while keeping the preceding and following mode shapes, (T⊕T)-1 and (T⊕T)+1 (), outside of that range.
- The T⊕T mode shape was constrained within 20±0.05 kHz in order to obtain a fine-tuned gigacycle biaxial specimen

- The biaxiality ratio k ($k = \frac{\sigma_1}{\sigma_2}$) obtained from the two principal stresses in the gauge area of the specimen was limited to a minimum of 0.8 ($0.8 \leq k \leq 1$).
-

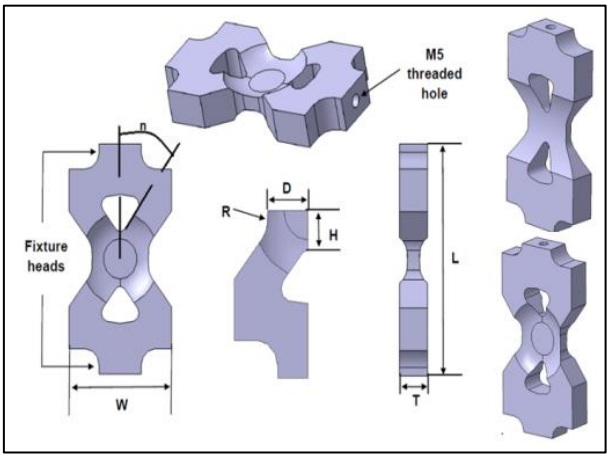

Figure1 Specimen optimised geometries

Results and discussion

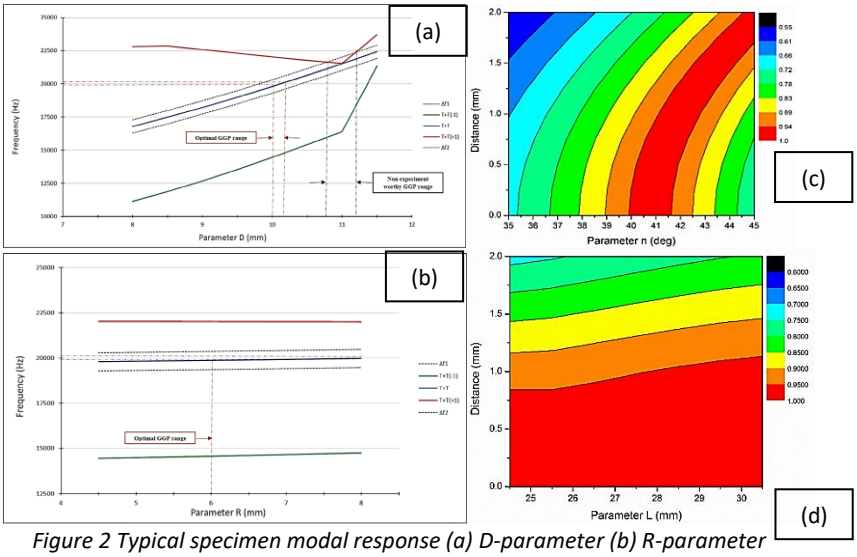

Figure 2 Typical specimen modal response (a) D-parameter (b) R-parameter Typical specimen biaxiality profile (c) n-parameter (d) L-parameter

From the modal response of the spherical and cylindrical specimens, it is possible to assess the sensitivity of the specimen to changing GGP values. The frequency gradient of the T⊕T mode shape gives an indication of the criticality of a GGP with regards to the modal response and an understating of their importance to achieve the modal ultrasonic test and specimen fine-tuning conditions. *Figure 2 (a) and (b)* exhibit respectively the influence trends of one highly influential parameter on the specimen response (D-parameter) and one parameter with a negligible impact on the modal response. The biaxiality profile of the specimen was assessed considering the uniformity of the biaxial stress state over the gauge area as well as the magnitude of the biaxiality factor ($0.8 \leq k \leq 1$). The influence of a GGP on the biaxiality was evaluated from the understanding of the stress gradient indicated by tightly-packed vertical contours for a high gradient (n-parameter in *Figure 2 (c)*) and loosely-packed horizontal contours for a low gradient (L-parameter in *Figure 2 (d)*). *Table 1* provides a summary of

the geometrical optimisation parameters for both the spherical and cylindrical specimens along with the optimal GGP value ranges to satisfy the three optimisation criteria established for a suitable gigacycle biaxial specimen.

Table 1 Specimen optimal value ranges

GGP (Spherical specimen)	Frequency gradient	Modal response optimal value ranges	Biaxiality optimal value ranges
D	1613 Hz/mm	[10.04 -10.10] mm	[8 – 11.5] mm
T	- 1378 Hz/mm	[4.90 – 4.97] mm	[4 – 7] mm
H	718 Hz/mm	[8.37 – 8.51] mm	[7.6 – 8.75] mm
L	- 526 Hz/mm	[26.11 – 26.30] mm	[24.5 – 30.5] mm
W	- 346 Hz/mm	[17.59 – 17.88] mm	[15 – 20] mm
n	- 138 Hz/degrees	[39.06 – 39.79] degrees	[37 – 44] degrees
R	51 Hz/mm	[7.53 – 9.48] mm	[4.5 – 8] mm
GGP (Cylindrical specimen)	**Frequency gradient**	**Modal response optimal value ranges**	**Biaxiality optimal value ranges**
D	1068 Hz/mm	[9.99 – 10.08] mm	[8 – 12.5] mm
T	-1019 Hz/mm	[5.03 – 5.13] mm	[4.65 - 7] mm
H	752 Hz/mm	[4.96 – 5.09] mm	[4.85 – 6] mm
L	-584Hz/mm	[25.73 – 25.90] mm	[24.5 – 30.5] mm
W	-344 Hz/mm	[17.75 – 18.04] mm	[15 – 20] mm
n	-256 Hz/degrees	[29.68 – 30.07] degrees	[25 – 30.5] degrees
R	34 Hz/mm	[2.23 – 5.16] mm	[4.5 – 8] mm

Conclusion

With a view to investigate, materials in the gigacycle fatigue range under a biaxial stress state, an optimisation process was carried out to produce two viable geometries for ultrasonic test specimens. Optimal value ranges for the geometrical governing parameters of the two specimens were obtained to allow the production of fine-tuned gigacycle biaxial specimens to be tested under the uniaxial excitation of an ultrasonic

References

[1] V. Kazymyrovych, “Very high cycle fatigue of engineering materials - A literature review,” Karlstad University Studies, 2009.

[2] H. Mughrabi and S. D. Antolovich, “A tribute to Claude Bathias – Highlights of his pioneering work in Gigacycle Fatigue,” *Int. J. Fatigue*, vol. 93, pp. 217–223, 2016.

[3] C. Brugger, T. Palin-Luc, P. Osmond, and M. Blanc, “A new ultrasonic fatigue testing device for biaxial bending in the gigacycle regime,” *Int. J. Fatigue*, vol. 100, pp. 619–626, 2017.

[4] M. Vieira, L. Reis, M. Freitas, and A. Ribeiro, “Strain Measurements on Specimens subjected to Biaxial Ultrasonic Fatigue Testing,” *Theor. Appl. Fract. Mech.*, 2016.

[5] D. Bellett, F. Morel, A. Morel, and J. L. Lebrun, “A biaxial fatigue specimen for uniaxial loading,” *Strain*, vol. 47, no. 3, pp. 227–240, 2011.

Development of enhanced power generation for piezoelectric energy harvesting

Nathan Counsell, Yong Chen, and Mohammad Reza Herfatmanesh

Centre for Engineering Research, School of Engineering and Computer Science, University of Hertfordshire

Energy harvesting is gaining significant interest from industry, which is driving research within this area. This interest has been attributed to the development of ultra-low-power electronics and the Internet of Things (IoT) [1]. The use of energy harvesting allows products to be relatively versatile for remote sensing applications. There are four major energy harvesting methods; inductive (electro-magnetic), thermoelectric, photo-voltaic and piezoelectric. All these methods except piezoelectric energy harvesting depend upon the use of batteries to store energy to power electrical devices. In the case of piezoelectric energy harvesters, significant instantaneous power can be generated, allowing for battery-less operation [2, 3]. Previous authors have investigated buckling structures for bi-stable cantilever structures [4-6]. This research investigates the effect of mono-stable buckling on the electrical output energy of a piezoelectric transducer. The investigation focused on the commercially available piezoelectric-ceramic; Lead Zirconate Titanate (PZT-5A), due to its low cost and high energy output which are crucial for commercial exploitation of the product. A bespoke punch and die tool was designed and manufactured to transform commercial piezoelectric transducers into mono-stable buckling energy harvesters. To characterise the buckling transducers, a bespoke clamp was designed and manufactured to provide simply supported clamping conditions on the edges of the piezoelectric transducers while a tensile machine with a point load was employed to measure the buckling force. The measured buckling force was then used to identify the output electrical energy produced by the buckled transducer. An important factor in assessing the performance of a mono-stable piezoelectric transducer is the height of the resulting curvature on the buckling structure. This study investigated the effect of curvature height, between 0.8mm and 1.4mm, on the required buckling force and the output energy of a 25mm circular PZT piezoelectric transducer. Empirical correlations have been developed to predict the buckling force and output energy of mono-stable piezoelectric transducers within the investigated curvature heights. The results demonstrated that the electrical output energy of a commercial PZT transducer increased significantly, from 261.3μJ to 576.0μJ, when converted into a buckling mono-stable state.

Reference

1. Yang, J., et al. A 2.5-V, 160-μJ-output piezoelectric energy harvester and power management IC for Batteryless Wireless Switch (BWS) applications. in VLSI Circuits (VLSI Circuits), 2015 Symposium on. 2015. IEEE.
2. Jung, W.-S., et al., Powerful curved piezoelectric generator for wearable applications. Nano Energy, 2015. 13(Supplement C): p. 174-181.
3. Uchino, K., Piezoelectric Energy Harvesting Systems—Essentials to Successful Developments. Energy Technology, 2018. 6(5): p. 829-848.
4. Syta, A., et al., Multiple solutions and corresponding power output of a nonlinear bistable piezoelectric energy harvester. The European Physical Journal B, 2016. 89(4): p. 1-7.
5. Jiang, X.-Y., H.-X. Zou, and W.-M. Zhang, Design and analysis of a multi-step piezoelectric energy harvester using buckled beam driven by magnetic excitation. Energy Conversion and Management, 2017. 145: p. 129-137.
6. Pan, D., Y. Li, and F. Dai, The influence of lay-up design on the performance of bi-stable piezoelectric energy harvester. Composite Structures, 2017. 161: p. 227-236.

A Gamified Prototype for Software Requirements Engineering

Helen Partou*, Catherine Menon, Trevor Barker and Vito Veneziano

Department of Computer Science, University of Hertfordshire, UK
*corresponding author: h.partou3@herts.ac.uk

Communication gaps remain a challenge for stakeholders involved in software Requirements Engineering (RE). Use of ambiguous emotive language is one example of complexity when eliciting requirements, which can lead to costly revisions if misrepresented. This paper presents the design of a gamified prototype application, which allows stakeholders to document and manage requirements. It includes customisation of De Bono's 'Six Thinking Hats' as a mechanism for gamification, and an emotive word bank to support stakeholder communication. The next phase of research proposed is an empirical study to assess impact of the prototype's features for RE.

Keywords: software requirements engineering; cognitive psychology; gamification; emotions; communication

Introduction

For software Requirements Engineering (RE), there remains ongoing challenges in eliciting and managing requirements for a development project. This is, in part, due to diverse stakeholders, such as the customer, requirements engineers, etc. Whilst there are communicative challenges with language and colloquialisms, there are also issues with ambiguity. For example, the use of emotive language, such as "surprise", has both positive and negative connotations. If this causes a communication gap in the context of RE, this can lead to costly revisions to requirements.

One technique which might help reduce communicative challenges is gamification. Whilst games are a fictional means of escapism, gamification refers to immersing game components into the real-world. This can spark competitive-collaborative dynamics into the everyday world of work, a concept which has been popularised in media, such as a song from Disney's 'Mary Poppins' [1]: "In every job that must be done / There is an element of fun / You find the fun and snap! / The job's a game".

Empirical studies [2] compared gamification with traditional (non-gamified) methods of requirements elicitation, suggesting that gamification might help elicit more requirements, though there were no major differences in emotions noted between methods. This paper presents a prototype application which allows stakeholders to document and manage requirements. It includes gamification, and an emotive word bank, to assess possible impact of these features for RE.

Prototype design elements I: De Bono's 'Thinking Hats' for RE gamification

In early prototype drafts, one stakeholder's home screen is in *Figure 1a*, and the requirements management screen in *Figure 1b*. Gamification features include stakeholder avatars, points with high scores and unlockable achievements. De Bono's 'Thinking Hats' [3], from the field of cognitive psychology, has been adapted as a means of gamifying RE and exploring its effects on cognitive load.

Stakeholders earn points from tasks linked to six coloured metaphorical hats: the **green** hat, representing creativity, for eliciting requirements as agile-based user stories; **yellow** hat for positive benefits and **black** hat for issues with requirements; **blue** hat for requirements prioritisation; **white** hat for neutral facts on the project and the **red** hat, symbolic of intuition, for expressing emotion.

Prototype design elements II: emotive word bank for communication

Another design element is the inclusion of a non-ambiguous emotive word bank based on the OCC (Ortony, Clore, Collins) 'Model of Emotions' [4], with the aim to support stakeholder communication.

In the prototype, an emotive word can be chosen (see *Figure 1c*) when sharing a benefit or issue with a requirement. When listed (see *Figure 1d*), these emotive words, such as joy or hate, are designed to help maximise communal understanding of the speaker's comments and intentions.

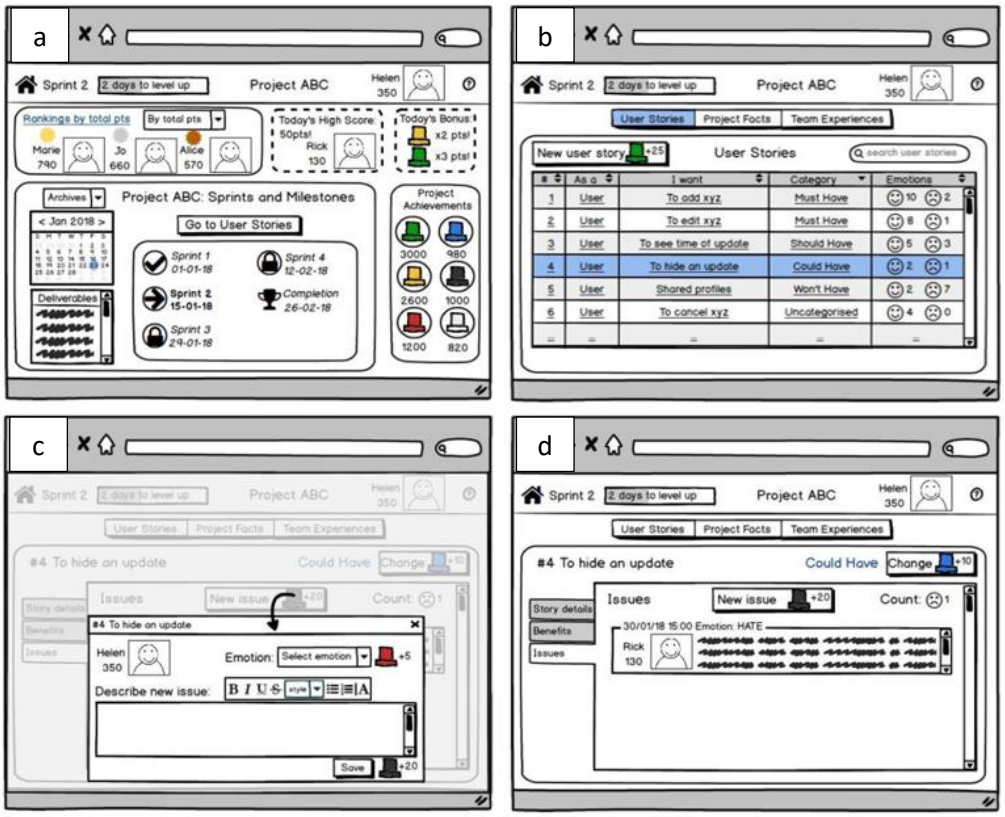

Figure 1. Early gamified prototype screens: (a) stakeholder homepage, (b) requirements management, (c) requirements issue with selection of emotive word, and (d) requirements issues listed with chosen emotive word

Next phase of research

To assess the impact of the prototype's features, an empirical study is proposed as the next phase of research. The study's design will need to minimise possible bias and isolate prototype features as a means of comparison between gamified and non-gamified methods. The measurements of impact could be based on two categories: 1) impact on requirements, such as number of requirements and revisions, and 2) impact on personal factors, such as comfortability and compassion.

Conclusion

RE faces ongoing challenges. Stakeholder communication gaps are one example acting against effective requirements validation. A gamified prototype based on De Bono's 'Thinking Hats', and an

emotive word bank, has been designed to explore whether such challenges can be minimised. An empirical study is the next phase proposed to assess impact of the prototype's features for RE.

Reference list

[1] Walt Disney Music Company, 'A Spoonful of Sugar', Mary Poppins [OST] (1964).
[2] Lombriser, P., Dalpiaz, F., Lucassen, G. and Brinkkemper, S., 'Gamified Requirements Engineering: Model and Experimentation', in *Proceedings of the Conference on Requirements Engineering: Foundation for Software Quality*, Switzerland: Springer, p. 171-187 (2016).
[3] De Bono, E., 'Serious creativity', *Journal for Quality and Participation* 18(5), p. 12-18 (1995).
[4] Ortony, A., Clore, G. and Collins, A., *The Cognitive Structure of Emotions*, Cambridge University Press: Cambridge (1998).

Session 2: Connect the people and cities

Session chaired by Dr Ian Johnston

Keynote: Interfaces and Concepts to Build Large Resilient and Predictable Systems

Raimund Kirner, Olga Tveretina

School of Engineering and Computer Science, University of Hertfordshire, Hatfield, UK
{r.kirner, o.tveretina}@herts.ac.uk

Progress in technology not only results in tools of improved capabilities, but also pushes towards integration to create larger systems with unprecedented capabilities. Building such systems with safety-relevant services demands appropriate system interfaces and algorithmic concepts. In this paper we list examples of ingredients to build large resilient and predictable systems.

keywords: resilience; predictability; large systems; system of systems; composability

1 Introduction

Building large systems is always a trade-off between the requirements and the available resources. One the rather large scale system examples is the internet, with more than one Billion websites. The internet has proven to be relatively resilient to different types of system faults or attacks. However, C.Hall et al. have analysed the resilience of the internet interconnection ecosystem in more detail, and concluded that the dependability of the internet has its limits [1]:

> *"The economics do not favour high dependability of the system as a whole as there is no incentive for anyone to provide the extra capacity that would be needed to deal with large-scale failures."*

While this is a valid design choice for the classical applications of the internet based on information exchange and data retrieval, there are an increasing number of large systems that would demand higher resilience than that provided by the internet interconnection ecosystem. For example, remote surgery would need communication lines with high availability between the hospital and the remote surgeon. Another example are smart cities, where we just stand at the beginning to envision what services are possible to make peoples' life more convenient and safe. In particular, safety-critical services are also envisioned, like the health monitoring and alerting for elderly people. To build such large systems with sufficient degree of resilience and predictability, we need to use adequate system interfaces and concepts. In this paper we provide some examples of what that can be.

2 Design Patterns for Large and Resilient Predictable Systems

In the following we introduce examples for systems design patterns that help to make systems for resilient and predictable.

2.1 Nearly Autonomous Systems

To design large systems, it is important to subdivide the system into subsystems, i.e., building a system of systems. To support resilience and predictability of critical services, it is important to design the corresponding subsystems providing that services as a *nearly autonomous system*. A nearly autonomous system is a subsystem with external communication that is able to provide its service even in the event of failure on the external communication channels. At the same time, it is recommended to use interfaces and algorithms that provide resilience against faulty data received on the external communication interface.

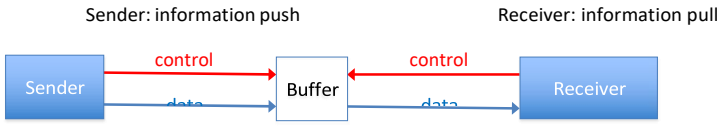

Figure 1. Push-Pull Communication Interface

An example for a resilient interface is the data exchange via a shared buffer, with decoupled write and read access. The sender controls when to write the data via an information push and the receiver controls when to read the data via an information pull [4]. This push-pull interface provides a temporal isolation between two subsystems. Such a communication interface supports composability as well as compositionality [7].

2.2 Interfaces for Mixed-Criticality Systems

Large systems tend to provide services of different criticality, where services of higher criticality have a higher weight for the overall system utility. To design such systems in a resilient and predictable way, it is also important to consider the message types and the type of message propagation [5]. For example, information exchange can be via event messages, state messages, or semi-state messages. State messages are preferred as they help to provide an immediate return to a consistent system state in case of erroneous failed communication. Communication channels of the system model have to be mapped to the physical communication medium. To provide fairness to the individual communication channels, approaches like bounded or time-triggered interfaces.

2.3 Lock-free Communication via the RNBC Protocol

Realising a push-pull communication as described in Section 2.1, it is also important to realise the access to the shared communication buffer with temporal decoupling. A way to achieve this is the *Rate-bounded Non-Blocking Communication* (RNBC) protocol [6]. The core principle of RNBC is to have lock-free communication with one writer and an arbitrary number of readers. RNBC is rather simple, with the implementation shown in Figure 2.a. However, the important property of RNBC is to have a formal schedulability criterion that ensures correct communication. As shown in Figure 2.b, RNBC uses a double buffer to ensure the reading of consistent data. With c_r, c_w being the worst-case execution time of the reader and writer code, and *mint* being the minimum inter-arrival time between two messages, the following schedulability criterion guarantees lock-free and consistent communication via RNBC:

$$c_w + c_r \leq mint$$

```
int buff[2];              // shared msg buffer

void rnbc write msg (int msg) {
   buff[wbuff] = msg;
   wbuff = 1−wbuff; // swap read / write
      buffer
}

int rnbc read msg () {
   int rbuff = 1−wbuff;
   return buff[rbuff];
}
```

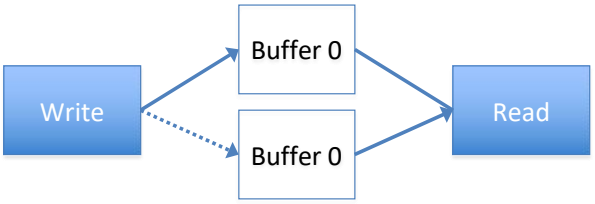

a) RNBC implementation b) RNBC double buffering

Figure 2. RNBC: Rate-bounded Non-Blocking Communication Protocol

2.4 Utility-based Service Optimisation

To design systems in a resilient way, we model the utility of individual services. Instead of using single design requirement limits like maximum delay or minimum throughput, we model these parameters via a utility function [3]. Figure 3 shows an example for modelling

the utility of the throughput of a service. Using these utility values of the individual services, we can optimise the overall system utility in case of a situation that causes a resource shortage [2].

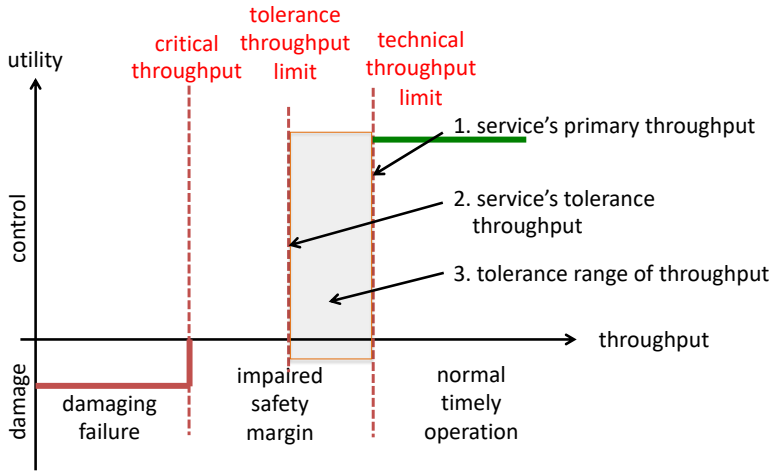

Figure 3. Service Utility Optimisation based on Throughput

3 Summary and Conclusion

In this research, we have made the case towards adequate system interfaces and concepts to achieve resilient and predictable large systems. We also listed a few examples of such system interfaces and concepts.

References

[1] C. Hall, R. Anderson, R. Claytona, E. Ouzounis, and P. Trimintzios. Resilience of the internet interconnection ecosystem. Summary report of ENISA study, European Network and Information Security Agency (ENISA), Apr. 2011. Available online at https://www.enisa.europa.eu/publications/interx-report.

[2] S. Iacovelli, R. Kirner, and C. Menon. ATMP: An adaptive tolerance-based mixed-criticality protocol for multi-core systems. In *Proc. 13th International Symposium on Industrial Embedded Systems (SIES'18)*, Graz, Austria, June 2018.

[3] R. Kirner. A uniform model for tolerance-based real-time computing. In *Proc. 17th IEEE Int'l Symposium on Object/Component/Service-oriented Real-Time Distributed Computing*, pages 9–16, Reno, Nevada, USA, June 2014.

[4] P. Puschner and B. Frömel. Composable component interfaces for time-triggered systems. *In Proc. 8th Mediterranean Conference on Embedded Computing (MECO'19)*, Jun. 2019.

[5] S. Maurer and R. Kirner. Cross-criticality interfaces for cyber-physical systems. In *Proc. 1st IEEE Int'l Conference on Event-based Control, Communication, and Signal Processing*, Krakow, Poland, June 2015.

[6] P. Puschner and R. Kirner. Interfacing to time-triggered communication systems. In *Proc. 22nd IEEE Int'l Symposium on Object/Component/Service-Oriented Real-Time Distributed Computing*, May 2019.

[7] P. Puschner, R. Kirner, and R. Pettit. Towards composable timing for real-time software. In *Proc. 1st International Workshop on Software Technologies for Future Dependable Distributed Systems*, Tokyo, Japan, Mar. 2009.

Data fusion in Internet of Things

Alok Verma*, Peter Lane, and Mariana Lilley
School of Engineering and Computer Science, University of Hertfordshire
* av17aas@herts.ac.uk

The Internet of Things (IoT) is set to become one of the key technological developments of our times. Sharing and collaboration of data and other resources will be the key to enabling sustainable ubiquitous environments, such as smart cities and societies. A timely fusion and analysis of data, acquired from IoT and other sources, to enable highly efficient, reliable, and accurate decision making and management of ubiquitous environments will play a key role in this development. The aim of this research is to design a context-aware data fusion framework for IoT with a focus on mathematical methods (Theory of Evidence).

Keywords: Context-aware; Data-Fusion; Dempster-Shafer; Internet of Things; Theory-of-Evidence

Introduction

There is a strong requirement to integrate multiple information sets in a dynamic environment like IoT. An open issue is to model and handle different kinds of uncertain information. This task is challenging predominantly due to the varied nature of IoT data streams [1, 2].

In this context, the research proposes a two-layered architecture for analyzing IoT data, using Dempster Shafer Theory (DST) [2] as a method for data fusion in IoT. The first layer provides an interface to store data from multiple sensors, analyze it and extract high-level events along with their associated probabilities.

The second layer is responsible for data fusion of these events. Here the state-of-the-art event processing is extended using DST, in order to account for the associated uncertainty while detecting these complex events. The solution is then demonstrated using a real-world case study in the domain of Intelligent Transportation Systems (ITS).

Experimental

Dempster- Shafer theory is a statistical approach for combining uncertain data where we cannot associate 100% probability to the certainty of the input data. It provides techniques to use and combine whatever certainty exists [2].

Given two Basic Probability Assignment (BPA) m1 and m2 which are obtained from two independent sources, an orthogonal sum [m1⊕ m2] is formulated in such a way that the sum is still a BPA [2].

$$[m_1 \oplus m_2](y) = \frac{\sum_{A \cap B = y} m_1(A) m_2(B)}{1 - \sum_{A \cap B = \emptyset} m_1(A) m_2(B)} \quad (1)$$

The following section demonstrates an example use of Dempster's combination rule in context of this research. Let the following frame of discernment describe the hypothesis space for the traffic predictions.

$$\Theta = \{\phi, \{N\}, \{CL\}, \{CG\}, \{N, CL\}, \{N, CG\}, \{CL, CG\}, \{N, CL, CG\}\}$$

Where N= Normal traffic, CG= Congestion, CL= Closed, and ϕ= null set. Two sensors $M_{Twitter}$ and M_{RSS} are providing information about traffic flow in the frame of discernment described above.

Table 1: Traffic data from sensors

	ϕ	N	CG	N, CG	CL	N, CL	CG, CL	N, CG, CL	Description
$M_{Twitter}$ (m_1)	0	0.1	0.4	0.05	0.1	0.05	0.2	0.1	Favours Congestion
M_{RSS} (m_2)	0	0.3	0.15	0.1	0.05	0.15	0.1	0.15	Normal Traffic

Results and discussion

Let M_{Both} represent a function that distributes combined mass for both the sensors.

Table2: Combined hypothesis space for both sensor data

Data Set	ϕ	N	CG	N,CG	CL	N,CL	CL,CG	CL,CG,N	Description
M_{Both}	0.0	0.22	0.43	0.034	0.151	0.046	0.093	0.023	Increased confidence in Congestion

As shown in Table 2, the values obtained after the computation assign more weight to {CG}, than the starting basic probability assignments do. There is a substantial loss of weight in {N}, as compared to initial mass distributions. The other elements of the power set Ω have net losses in weight except for {CL}. The degree of belief in the proposition {CG} is substantially higher than that based on initial values from $M_{Twitter}$ 0.4 and M_{RSS} 0.15. The degree of belief in the powerset Ω (M_{Both}), remains unchanged and is equal to 1.

Conclusion

Expressivity of the frame of discernment allows us to gain insight into the role played by each input feature and to interpret hidden influences in the data fusion process. The experimental results show that the proposed data fusion framework is efficient in handling conflicting pieces of evidence from various heterogeneous sources.

Reference list

[1] F. Alam, R. Mehmood, I. Katib, N. N. Albogami, and A. Albeshri, "Data Fusion and IoT for Smart Ubiquitous Environments: A Survey," *IEEE Access*, vol. 5, pp. 9533–9554, 2017.

[2] G. Shafer, *A mathematical theory of evidence*. Princeton University Press, 1976.

[3] P. Mehrannia, A. A. Moghadam, and O. A. Basir, "A Dempster-Shafer Sensor Fusion Approach for Traffic Incident Detection and Localization," in *2018 21st International Conference on Intelligent Transportation Systems (ITSC)*, 2018, pp. 3911–3916.

Numerical Methods for the Thermal Design and Analysis of Airframe Structures for High Speed Aerospace Vehicles

Paul Canoville

University of Hertfordshire, School of Engineering and Computer Science, Hatfield, UK

MDBA, Stevenage, UK

This research is concerned with developing numerical methods applicable for the thermal design and analysis of airframe structures for the scramjet propulsion powered Hypersonic Air-breathing Weapon Concept HAWC (i.e Mach 5+ cruise missiles). Computational Fluid Dynamics (CFD) methodology is being used to develop the vehicle airframe aerothermal environment prediction capability with the ANSYS Fluent tool [1]. A major source of uncertainty in the computation of aerothermal environments for air breathing vehicles is often governed by inadequacies in the turbulence models employed in CFD methods particularly at locations of the airframe that encounter Shock-Wave Boundary Layer Interactions (SWBLI). The main emphasis of the research to date has been focused on undertaking a set of canonical unit test cases to evaluate the best performing turbulent model candidates available in the Fluent tool for predicting wall surface quantities of interest (Q of I) (i.e. heat flux, shear stress, pressure) at SWBLI. The Spalart-Allmaras (SA) 1 equation model [2] and k-ω Menter SST two equation model [3] were identified as the strongest performing candidates to take forward into the research program. The research is now focused on further optimising the selected RANS turbulent model candidates to further confidence in prediction capability of the CFD method, particularly at SWBLI regions.

Keywords: CFD; Hypersonic air breathing vehicle; Shock-wave boundary layer interaction; turbulence modelling.

Introduction

During flight hypersonic vehicles are impacted by severe aerothermal environments characterised by strong shocks and high temperatures that result in severe heating of the vehicle. Thermal protection systems (TPS) [4] are therefore required to ensure safe operation of the vehicle. The severity of the aerothermal environment impacting hypersonic vehicles in flight primarily depends on the vehicle configuration (blunt vs sharp, surface features etc.) and mission profile. At one end of the spectrum re-entry vehicles encounter an aerothermal environment dominated by high enthalpy flow that is processed by the bow shock leading to elevated levels of ionisation that result in significant radiative heating and high-heat shield ablation. At the other end of the spectrum, air breathing vehicles fly at lower altitudes and in high dynamic pressure where the aerothermal environment is dominated by fluid dynamic effects including - transition, turbulence and shock interaction. The design and safe operation of hypersonic vehicles requires adequate definition of the aerothermal design loads to specify the TPS of the vehicle. Aerothermal environment design loads cannot be solely obtained from ground-test facilities because no facility can reproduce all aspects of the flight environment. This limitation is particularly true for hypersonic flight where very high energy is required to create a representative hypersonic environment at a reasonable scale on the ground. Numerical predictive methods therefore have a vital part to play in the contribution to the development of hypersonic vehicle technology. Methods developed in this research will be applicable to all areas of the vehicle external airframe including aerodynamic control surfaces and inlet and isolator regions of the air breathing propulsion device. CFD methodology is being used to develop the vehicle airframe aerothermal environment prediction capability. A major source of uncertainty in the computation of aerothermal environments for air breathing vehicles is often governed by inadequacies in the turbulence models employed in CFD methods particularly at locations of the airframe that encounter SWBLI. These interactions usually lead to localised heating rates that are much higher than the surrounding areas. Reliable prediction of surface heat flux at these interaction regions is therefore of vital importance for the successful design of the airframe TPS.

Method

The ANSYS Fluent solver is being used to develop the CFD method for this research. The fundamental governing equations employed in the CFD method are based on solution of the finite volume formulation of the Reynolds Averaged Navier Stokes (RANS) equations. The inviscid fluxes embedded in the governing equations are computed using the Advection Upstream Splitting Method (AUSM+) flux vector splitting scheme [5] and an implicit solver scheme is used to solve the discretized equation set [6]. The CFD method will be coupled to a numerical method structural thermal response tool to develop full simulation capability to cover 'passive' (i.e hot structure, insulation, heat sink) vehicle airframe TPS [4] approaches for flight within the continuum air region of the earth's atmosphere.

Results and discussion

A set of unit test cases to down select the strongest performing RANS 1 and 2 equation turbulent model candidates available in the Fluent tool has been undertaken. Performance metrics used to determine best turbulent model candidates included comparison against experiment data obtained for predicted location and value for peak wall surface Q of I and shock interaction region separation bubble size. The experiment data compared against in the unit test cases undertaken are derived from measurements made over simple planar and axisymmetric configurations. Nevertheless, these configurations induce complex regions of the SWBLI, separated flows etc. typically encountered over the airframe of hypersonic air breathing vehicles during flight, that a stringent test for the turbulence modelling employed in the CFD method is provided. An illustrated example of a unit test case undertaken showing predicted surface heat flux results obtained as compared to experiment data for each turbulent model candidate evaluated is presented in the following Figure (1).

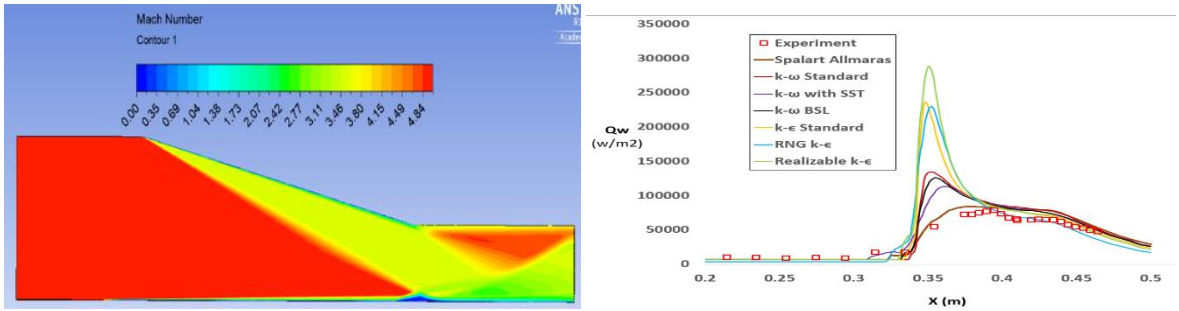

Figure 1. 2D impinging shock unit test case configuration at Mach = 5.0, Re/m = 4.9 x 10^6. Experiment data taken from [7].

Conclusion

The Spalart-Allmaras (SA) 1 equation model [2] and k-ω Menter SST [3] two equation model were identified as the strongest performing candidates to take forward into the research program. The research is currently focused on further optimising the selected RANS turbulent model candidates to further confidence in prediction capability of the CFD method, particularly at SWBLI regions. This includes investigating the utility of anisotropic turbulent models [8], turbulent length scale and compressibility source term [9] formulations through development of 'C' source code User Defined Functions (UDF) that will be loaded with the Fluent solver.

Reference list

[1] http://www.ansys.com/Products/Fluids/ANSYS-Fluent.

[2] P. Spalart and S. Allmaras. “A one-equation turbulence model for aerodynamic flows" Technical Report AIAA- 92-0439. 1992.
[3] F.R Menter. “Two-equation eddy-viscosity turbulence models for engineering applications”. AIAA Journal, Vol. 32, 1994.
[4] D.E. Glass. “CMC Thermal Protection Systems and Hot Structures for Hypersonic Vehicles”. AIAA-2008-2682, 2008.
[5] K.H Kim, C. Kim, O. Rho, “Methods for the accurate computations of hypersonic flows”. Journal of Computational Physics, 174, 38-80, 2001.
[6] J.M Weissi, W.A Smith, “Implicit solution of the navier stokes equations on unstructured meshes”. AIAA-97-2103, 1997.
[7] E. Schullein, “Skin-friction and heat flux measurements in SWBLI flows”. AIAA Journal, Vol. 44, No. 8, August 2006.
[8] H. Loyau. “Modelling SWBLI with Nonlinear Eddy-Viscosity Closures”. Flow, Turbulence and Combustion 257–282, 1998.
[9] D.C. Wilcox. “Turbulence modelling for CFD”. Chapter 5. D C W Industries, 3rd edition, July 2006.

Software Defined Networking for 5G compatible Enhanced WiFi Video Broadcasting

Matthew Robinson[1*]
[1]*University of Hertfordshire*
*corresponding author: m.robinson20@herts.ac.uk

In this work an SDN testbed was emulated in real time with direct WiFi access point attachments, real WiFi-connected End Users that ran custom live video receiving Applications (EUA), and a live SatIP video feed that injected multicast IPTV packets. Additional Forward Error Correction (FEC) packets were sent in parallel to offset the errors inherent in WiFi broadcasts; the FEC usage rate was calculated by the EUA and fed-back to the SDN controller in real time. Our SDN controller used this information to change the network's routing protocols, reducing the used multicast bandwidth by 38% in our tested scenario.

Keywords: WiFi multicasting; Video; 5G; Software defined networking; IPTV

Introduction

Data delivery trends show video is being consumed at ever increasing rates. Internet Protocol (IP) video traffic is set to account for 82% of all traffic by 2022 [1]. Additionally, traffic from wireless and mobile devices are predicted to account for 71% of the total IP global traffic by 2022 [1]. Software defined networking (SDN) is a prevalent technique being employed in the design of Fifth Generation (5G) networks and architectures to meet the newly founded International Mobile Telecommunications-2020 (IMT-2020) requirements for <1ms latency and user experienced data rates >100 Mbps [2]. This clear shift towards video consumption on mobile devices means that as well as fulfilling the IMT-2020 requirements, the demand for video delivery will also need to be designed for in 5G networks. This work aims to enhance current video delivery methods for fixed wireless access networks with the use of SDN in a way that is compatible with 5G Network Function Virtualised (NFV) techniques [3]. A key technique being described in literature is fixed wireless access network video offloading, wherein a local source for video content is used instead of an internet-based source. This allows the bandwidth that is saved on the backhaul network to be used for other applications; enhancing user experience and reducing operator cost [4].

The objectives of this work were to produce a system that can deliver a variable FEC multicast video service over WiFi that leverages the benefits of SDN networks to reduce the multicast bandwidth needed in the system, for an offloaded service; in this case, SatIP.

Experimental Setup

An SDN topology was emulated using Mininet on a Linux workstation [5]. Within this topology Open vSwitch and virtual Ethernet pairs were used to create a distribution network between 5 hardware Ethernet ports [6]. These Ethernet ports were connected to the SatIP server, the DHCP/Router, and 3 WiFi access points. Within the network, the SatIP server was connected directly to a Virtual Network Function (VNF) designed to split the FEC packets into different destination addresses. The output of the VNF was sent into the SDN topology. The 3 WiFi access points were

connected to end users' (mobile phone or tablets) that ran a custom written video client application. On top of the SDN topology a Pox SDN controller was installed with a custom SDN application, connected via the localhost [7]. This application was designed to calculate the amount of FEC required by the end users, based on their feedback, and update the network in real time so-as-to only deliver the required amount. This setup can be seen in Figure 1.

Results and discussion

By default, an error rate of 40% is assumed and used for FEC generation in non-variable deployments of the SatIP system. Based on this assumption approximately 35 UDP FEC packets are generated and sent per video cycle. In Figure 2 the amount of FEC required over time by the end users as calculated by the SDN controller based on real-time feedback can be seen per WiFi access point. In Figure 2, it can be seen that the amount of FEC required varies for each access point, as the end users connected to them are in different wireless environments. Overall, the SDN application can apply a reduction of 70% for the FEC specific UDP packets, which equates to a reduction of 38% for all multicast traffic in the scenario.

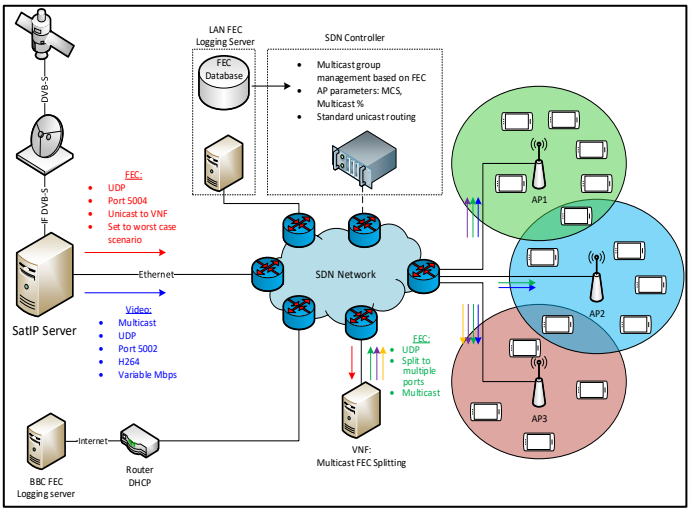

Figure 1. SDN enabled SatIP FEC Topology.

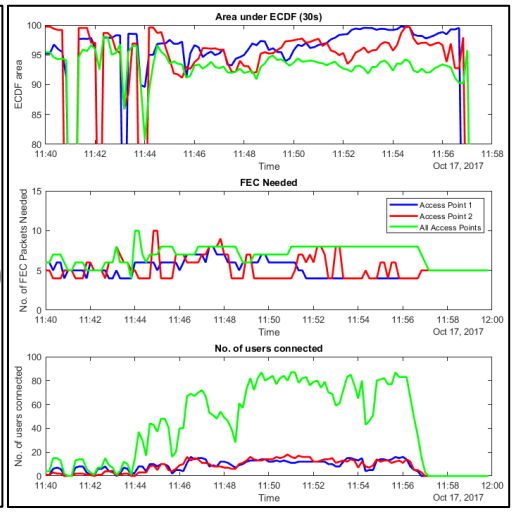

Figure 2. FEC results per access point.

The algorithms used in this work can be used in other areas of wireless communication including SDN enabled 4G and 5G networks. In addition, the same technique can be applied to much larger topologies, such as campus or enterprise networks with more than one source. Intelligent routing will allow access points to be connected to different sources using the most efficient route, while still ensuring a high Quality of Experience for end users.

Conclusion

This work has presented a new scheme for allowing adaptive FEC for wireless networks through the use of Software Defined Networking and custom written applications. For the scenario presented, a reduction of 38% for multicast traffic was made, while still allowing faultless video playback to end users.

Reference list

[1] CISCO, "Cisco Visual Networking Index: Forecast and Trends, 2017–2022," 2018.
[2] ITU, "IMT Vision – Framework and overall objectives of the future development of IMT for 2020 and beyond," ed. 2016.
[3] J. G. Andrews, S. Buzzi, W. Choi, S. V. Hanly, A. Lozano, A. C. K. Soong, et al., "What Will 5G Be?," IEEE Journal on Selected Areas in Communications, vol. 32, pp. 1065-1082, 2014.
[4] X. Zhang and Q. Zhu, "Scalable Virtualization and Offloading-Based Software-Defined Architecture for Heterogeneous Statistical QoS Provisioning Over 5G Multimedia Mobile Wireless Networks," IEEE Journal on Selected Areas in Communications, vol. 36, pp. 2787-2804, 2018.
[5] Mininet, website: http://mininet.org/, visited 12/06/2019.
[6] Open vSwitch, website: https://www.openvswitch.org/, visited 12/06/2019.
[7] Pox, website: https://github.com/noxrepo/pox, visited 12/06/2019.

Session 3: Protect and Care

Session chaired by Dr Volker Steuber

Keynote: Fluorescence visualisation to evaluate effectiveness of personal protective equipment for infection control

Brian Crook*, Samantha Hall
Health and Safety Executive Science and Research Centre, Buxton SK17 9JN , UK
*corresponding author: brian.crook@hse.gov.uk

In some instances healthcare workers will rely on personal protective equipment (PPE) to prevent exposure to potentially infective body fluids from patients with high consequence infectious diseases (HCID). To provide an evidence base to evaluate PPE ensembles, a simulation of a clinical procedure was developed using a mannequin and body fluid simulants with fluorescent markers. This was used successfully to evaluate a range of PPE ensembles and identify breaches of PPE. It led to the development of a unified PPE ensemble, shown to be fully protective, to be adopted by all UK hospitals designated to care for HCID patients.

Keywords: healthcare; infectious disease; personal protective equipment; fluorochrome; clinical simulation.

Introduction

The outbreak of Ebola Virus Disease (EVD) in West Africa in 2014-15 not only claimed thousands of lives, it also emphasised the potential infection risk for healthcare workers (HCW) coming into contact with contaminated body fluids. Unfortunately, this is currently being repeated in the Democratic Republic of Congo where a significant number of HCW have been infected.

In 2015, in response to the possibility of travellers returning to the UK from countries affected with EVD infection, contingencies were put in place including health checks and surveillance at entry points, and patient care capability. The latter was primarily focused on the High Level Isolation Unit facilities at the Royal Free Hospital in London, where patients can be cared for in 'Trexler' isolation beds which provide a physical barrier between the patient and the HCW. These were used successfully on the occasions they were required. However, if patients could not be treated in such facilities, or if patient numbers exceeded capacity at the HLIU, specialist High Consequence Infectious Disease (HCID) units were established at a network of hospitals in England (Newcastle, Liverpool and Sheffield) supplemented by a hospital in Glasgow with previous practical experience in caring for patients with viral haemorrhagic fever. These HCID units however do not have Trexler facilities, so HCW must rely on personal protective equipment (PPE) to provide protection from infection risk both during initial assessment and during continued care. For the initial assessment of a patient suspected to have a HCID, each unit developed PPE ensembles to complement their working practices, HCW skills and experience, and available PPE equipment, which led to some differences. To address these differences and work towards the development of a unified PPE ensemble, objective tests were devised around a simulation of clinical procedures and using Ultraviolet (UV) fluorochromes in simulated infectious body fluids.

Experimental

UV fluorescent dyes were added to body fluid simulants such that each was visible under UV light with a different colour – blue for "vomit"; red for "cough" (both simulants made up in water); orange in a glycerol mixture to simulate sweat and green in a flour/oil/salt/water mixture to simulate diarrhoea. A clinical skills education mannequin was adapted to deliver these body fluid simulants [1]. "Vomit"

was delivered via a compressed air driven piston and liquid reservoir previously used to simulate projectile vomiting to mimic Norovirus infection [2, 3] and connected into the mannequin's mouth. "Cough" was delivered via an airbrush fitted into the lower jaw of the mannequin; "sweat" was manually spread on the limbs before each simulation exercise and "diarrhoea" was placed on a pad beneath the mannequin. In the exercise, a doctor and nurse pair of volunteers conducted a clinical examination of the mannequin as they would a patient with suspected HCID, while wearing the appropriate PPE ensemble. During the examination they therefore came into direct contact with the body fluid simulants, or indirectly through the cough spray operated remotely, and the exercise culminated in the mannequin "projectile vomiting" to expose the volunteers. After the exercise, volunteers were examined under in a UV light unit [4], body mapped and photographed to locate contamination on their PPE. After removal using a standardised doffing protocol they were re-examined under UV to visualise any cross- contamination.

Results and discussion

Using this simulation exercise, five different PPE ensembles (Fig 1a) were evaluated [5]. In summary, cross-contamination events were evident in some instances which could be attributed to PPE failures or doffing errors (an example in Fig 1b and c).

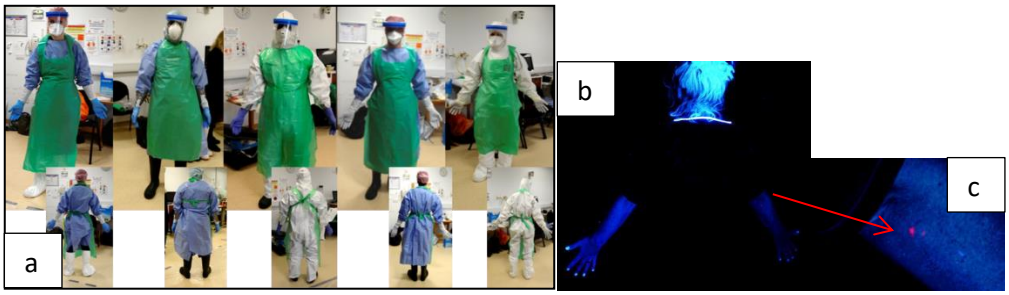

Figure 1. PPE ensembles tested (a), example of cross-contamination on arm (b), in close up in (c)

Based on the results where cross-contamination was evident, a unified PPE ensemble was developed as a consensus agreement between the HCID units. This was tested by repeating the exercise described above and found to be completely protective [6].

Conclusions

A simulation of clinical procedures was possible using a clinical training mannequin. By adapting it to expose HCW to body fluid simulants with fluorochrome markers and using UV visualization, it was possible to provide an evidence-based evaluation of PPE ensembles. This led to a unified PPE ensemble which is being adopted by all HCID units

References

[1] Poller B, Hall S, Bailey C et al, J Hosp Infect **99**, 229-235. (2018). Doi: 10.1016/j.jhin.2018.01.021.
[2] Crook B, Makison Booth C, and Hall S, Int J Pub Health Safe **3;2**, 156. (2018).
[3]Makison Booth C, J Infect Prev **15**, 176–80. (2014). Doi: 10.1177/1757177414545390
[4] Roff MW, Ann Occup Hyg **41**, 313-324. (1997).
[5] Hall S, Poller B, Bailey C et al, J Hosp Infect **99**, 218-228. (2018). Doi: 10.1016/j.jhin.2018.01.002.
[6] Poller B, Tunbridge A, Hall S et al, Journal of Infection **77**, 496–502. (2018) https://doi.org/10.1016/j.jinf.2018.08.016

Development of a fieldable autonomous optical detection system for the detection of waterborne pathogens

R Kaye[1*], I Johnston[1], D McCluskey[1], M Tracey[1], I Munro[1], Y Wang[1], B Suckow[2], I Klaholz[2]
[1]Microfluidics and Microengineering Research Group, University of Hertfordshire, Hatfield, AL10 9AB, UK
[2]ttz Bremerhaven, Am Lunedeich 12, 27572 Bremerhaven, Germany
*corresponding author: r.kaye2@herts.ac.uk

Disease outbreaks caused by long-known and emerging pathogens have a huge impact economically in aquaculture. Betanodavirus and E. Coli are the primary culprits with up to 100% mortality rate in fish from the former, and human health impacts from the latter. To address this, UH have developed a fluorescence based pathogen detection unit utilising microfluidics and optics that can be operated as an early warning system for waterborne pathogens. It is hoped with further development this could be a very useful tool for prevention of biosecurity breaches, environmental monitoring in key regions, and assisting early response protocols.

Keywords: Bio-detection; Aquaculture; Pathogens; Sustainability; Bio-security

Introduction

Every year the aquaculture industry is faced by disease outbreaks caused by long-known and emerging pathogens. Some of these pathogens have the capacity to heavily affect the sustainability of the business, while others can chronically affect the stocks, reducing the efficiency of the farming operation. The main species of pathogens affecting the Mediterranean industry comprise parasites, bacteria and viruses with the latter ones being the most difficult and expansive to detect. E. Coli and Betanodavirus are primary threats [1]. An outbreak of Viral Nervous Necrosis (VNN; caused by Betanodavirus) causes high mortality [2] and subsequently involves halting of operations, quarantining sites and culling of stock thus having a significant economic impact through direct losses, inhibition of trade and restriction on locations suitable for aquaculture expansion.

Figure 1: CAD render of pathogen detector (Top left), Fluidics and electronics layout of sensor (Top right), Flow cell design for pathogen sensor (Bottom).

The aims of this project were therefore to develop a fieldable autonomous pathogen detection system. The device was to target pathogens relevant to European waters, provide highly accurate in-situ measurements, detect pathogens at low concentrations in seawater, and run autonomously with human intervention limited to changing fluids required for operation and replacing the microfluidic

chip when necessary. UH have developed a fluorescence-based pathogen detection unit (Fig 1) that can be operated as an early warning system for waterborne pathogens. Consideration was given to several subsystems during the design and development regarding fluidics, optical detection, mechanical design, and the interaction with environmental sample.

Development

The development of the pathogen detection system focused on several key subsections: Optical detection system, fluidic handling system, and mechanical design.

For the optical detection of pathogens, aptamers biologically labelled with a quencher and fluorophore (DY-521XL) were used to provide a quantifiable signal indication a binding event of a pathogen. The system utilizes a 520 nm laser as an excitation wavelength and bandpass filters in a confocal optical set-up for the detection of the fluorophore emission wavelength (668 nm) using an photomultiplier tube.

The fluidics design was developed to accommodate the changes made to the bioassay over the course of the project, including the introduction of washing step and use of anti-bodies as a secondary stage in a sandwich assay.

The entire system was designed to operate in a custom light tight 19” rack mountable chassis. The flow cell itself was designed to move linearly and autonomously over the optics to enable multiple readings to be taken over the length of the flow cell.

Testing

There were numerous testing stages to ensure the optical set-up would perform adequately at low low fluorophore amounts. These tests included material autofluorescence testing in order to select the best suited material for use in the flow cell assembly. The results of these tests showed that although COC Topas plastic showed promise in terms of birefringence according to the literature, PMMA performed better with a background signal 25% that of COC as a result of autofluorescence. As a result the flow cell was manufactured using PMMA.

Tests were run using aptamer bound to the flow cell surface with a fluorophore at varying deposit amountsto try to find the limits of detection. The results from this indicate detection events down to deposits of 0.1 pmol.

Conclusions and Future Work

The system was able to successfully detect aptamers bound to fluorophores on the surface of the flow cell down to amounts of 0.1 pmol. This is not a limit and there is room to reduce this amount of fluorophore further and still get a discernable signal. Changes were made to the system during the project which included removing the quencher from the aptamer and running a sandwich assay with a secondary antibody bound to a fluorophore to detect the presence of a pathogen. This work is still in development and further work is needed on the bio-assay as non-specific binding events have made it difficult to accurately determine real binding events.

Reference list

[1] B L Munday, J Kwang, N Moody, Journal of Fish Diseases **25**, 127-142 (2002)
[2] S C Chi, C F Lo, G H Kou, P S Chang, S E Peng, S N Chen, Journal of Fish Diseases **20**, 185-193 (1997)

Sparse Coding with a Somato-Dendritic Learning Rule

Damien Drix[123], Verena V. Hafner[23], and Michael Schmuker[13]

[1]Biocomputation group, Department of Computer Science, University of Hertfordshire, United Kingdom
[2]Adaptive Systems laboratory, Institut für Informatik, Humboldt-Universität zu Berlin, Germany
[3]Bernstein Center for Computational Neuroscience, Berlin, Germany

Cortical neurons are silent most of the time. This sparse activity is energy efficient [1], and the resulting neural code has favourable properties for associative learning. Most neural models of sparse coding use some form of homeostasis to ensure that each neuron fires infrequently [2]. But homeostatic plasticity acting on a fast timescale may not be biologically plausible [3], and could lead to catastrophic forgetting in embodied agents that learn continuously.

We set out to explore whether inhibitory plasticity could play that role instead, regulating both the population sparseness and the average firing rates. We put the idea to the test in a hybrid network where rate-based dendritic compartments integrate the feedforward input, while spiking somas compete through recurrent inhibition. A somato-dendritic [4] learning rule allows somatic inhibition to modulate nonlinear Hebbian learning in the dendrites. Trained on MNIST digits and natural images, the network discovers independent components that form a sparse encoding of the input and support linear decoding.

These findings confirm that intrinsic plasticity is not strictly required for regulating sparseness: inhibitory plasticity can have the same effect, although that mechanism comes with its own stability-plasticity dilemma.

Going beyond point neuron models, the network illustrates how a learning rule can make use of dendrites and compartmentalised inputs; it also suggests a functional interpretation for clustered somatic inhibition in cortical neurons.

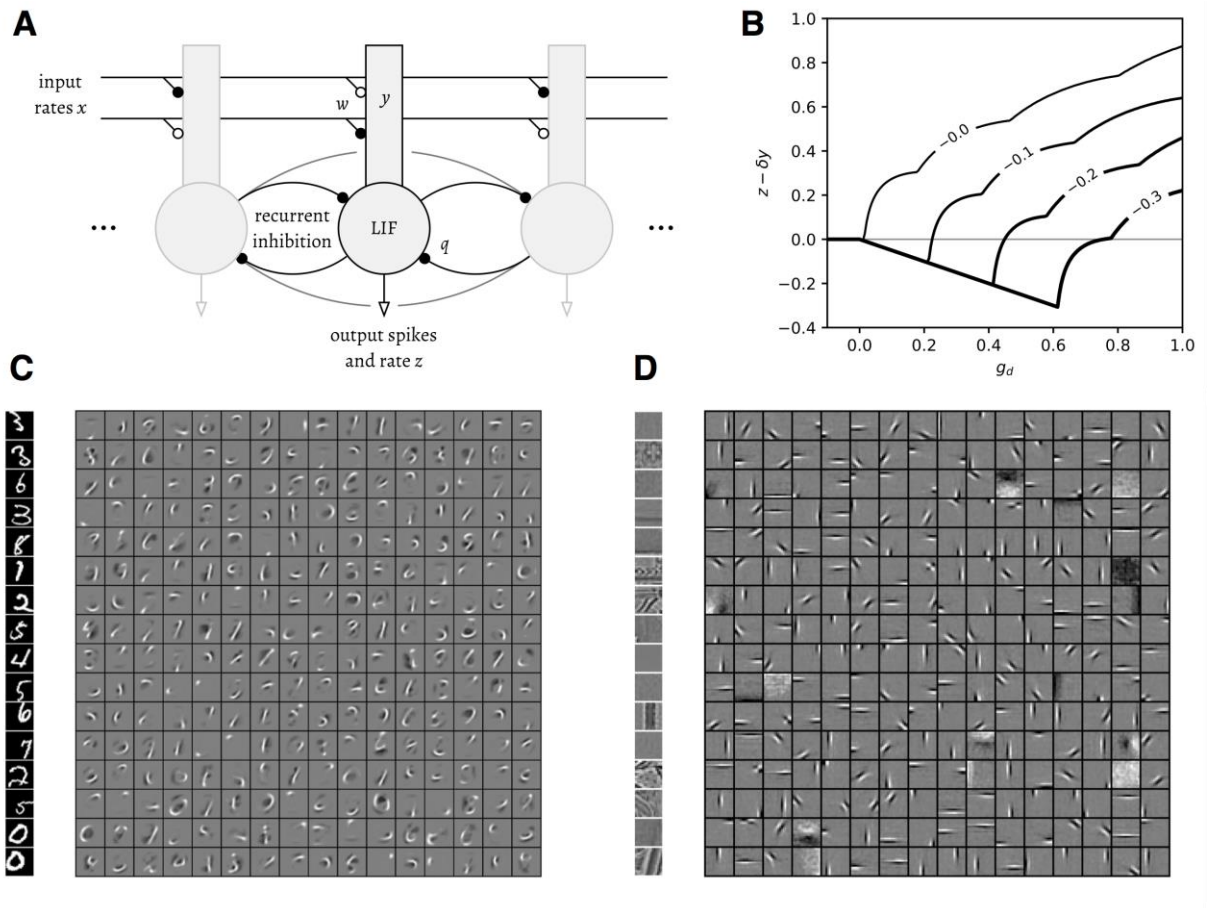

A Architecture of the network. **B** The learning rule results in an effective Hebbian nonlinearity where the change of weight *(y axis)* varies as a function of the dendritic activation *(x axis)* and the somatic inhibition *(number on curves)*. **C** The network learns pen-stroke shapes from MNIST digits. **D** The network learns oriented edges and broad gradients from whitened natural images.

[1] Olshausen, B. A. and Field, D. J., Vision Research 37(23), pp. 3311–3325 (1997).
[2] Földiák, P., Biological Cybernetics 64, pp. 165-170 (1990).
[3] Toyoizumi, T., Kaneko, M., Stryker, M. P., and Miller, K. D., Neuron 84(2), pp. 497–510 (2014).
[4] Urbanczik, R. and Senn, W., Neuron 81(3), pp. 521–528 (2014).

Investigating activity dependent dynamics of synaptic structures in biologically plausible models of post-deafferentation network repair

Ankur Sinha[1*], Christoph Metzner[2], Neil Davey[1], Roderick Adams[1], Michael Schmuker[1], and Volker Steuber[1]

[1]UH Biocomputation Group, CCSIR, University of Hertfordshire, UK

[2]Department of Software Engineering and Theoretical Computer Science, Technische Universitat Berlin, Berlin, Germany

*corresponding author: a.sinha2@herts.ac.uk

The brain retains its capacity to form and remove synapses in adulthood. This type of plasticity, termed structural plasticity, can alter the connectivity, and therefore the function, of neuronal networks of the brain over periods of days and months. Homeostatic structural plasticity in the brain has been studied extensively using neuronal imaging studies. We have developed a new model of peripheral lesioning and structural plasticity in a biologically realistic spiking neural network to investigate the underlying mechanisms that drive these changes.

Keywords: structural plasticity, homeostatic plasticity, brain repair, computational modelling

Introduction

It is now well established that the brain retains its capacity to form and remove synapses in adulthood. This type of plasticity, termed structural plasticity, can alter the connectivity and, therefore, the function of neuronal networks of the brain over periods of days and months [1]. Several lesion experiments have described alterations of synaptic structures during network reorganization by homeostatic structural plasticity in detail. The underlying mechanisms that drive these changes, however, are yet to be explained [2]. To investigate the reorganization of synaptic structures reported in these lesion studies, we simulated a peripheral lesion in a biologically plausible cortical spiking network model that exhibits asynchronous irregular (AI) firing [3]. Here, we present results from our computational modelling study.

Experimental

Our model consists of populations of excitatory (E) and inhibitory (I) spiking neurons distributed in a rectangular grid. Apart from inhibitory synapses from I neurons to E neurons (IE synapses), which have conductances that are modulated by the Vogels-Sprekeler asymmetric Spike Timing Dependent Plasticity (STDP) [3], all other synapses (EE, EI, II) are static. We extend a previous model of structural plasticity (MSP) [4] to implement activity dependent formation and removal of synaptic collaterals in the neurons of the network. The structural plasticity mechanism acts on all synapses and changes the synaptic connectivity of the network.

The network is first permitted to settle into its physiological AI regime under the action of the homeostatic synaptic plasticity mechanism. A peripheral lesion is then modelled in the network by deafferenting a subset of neurons to form the lesion projection zone (LPZ). The homeostatic structural plasticity mechanism is then allowed to restore activity to the deprived neurons and re-establish its pre-deafferentation steady state.

Results and discussion

Results from our simulations suggest that for activity to be restored to deprived neurons in the lesion projection zone (LPZ), excitatory and inhibitory post-synaptic structures must exhibit opposite activity dependent growth behaviors. An analysis of these growth regimes indicates that they contribute to the maintenance of optimal activity levels in individual neurons. Where a reduction in neuronal activity results in the sprouting of new excitatory post-synaptic structures, it is accompanied by the retraction of their inhibitory counterparts. Extra activity is similarly countered by a retraction of excitatory post-synaptic structures and sprouting of inhibitory ones. Our simulations also reproduce the ingrowth of excitatory axons into, and the outgrowth of inhibitory axons out from the LPZ that have been observed in lesion experiments. We find that the ingrowth of excitatory axons requires that sprouting of excitatory pre-synaptic structures is stimulated by extra excitatory neuron activity. The outgrowth of inhibitory axons, on the other hand, necessitates the sprouting of inhibitory pre-synaptic structures to be prompted by a loss in inhibitory neuron activity.

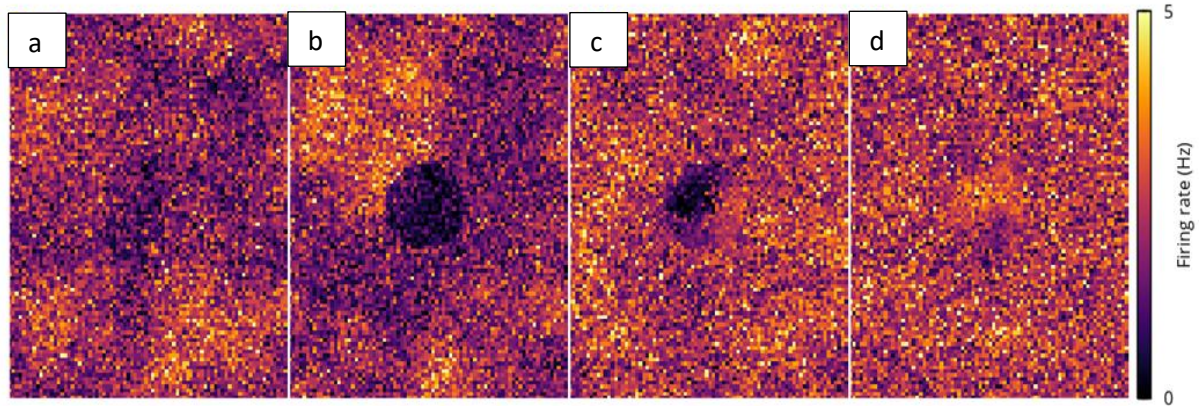

Figure 1. Firing rates of the excitatory population at different stages of the simulation: (a) before deafferentation; (b) after deafferentation; (c) during repair; (d) after repair.

Conclusion

We have developed a new computational model of peripheral lesioning and structural plasticity to investigate the role of homeostatic structural plasticity in the network repair process. By closely reproducing the reorganization of the network after deafferentation as observed in biological experiments, we make testable predictions about the activity dependent dynamics of synaptic structures.

Reference list

[1] Butz, M. and van Ooyen, A., BMC Neuroscience **15**, p17 (2014).
[2] Sammons, R. P. and Keck, T., Current Opinion in Neurobiology **35**, p136-141 (2015).
[3] Vogels, T. P., Sprekeler, H., Zenke, F., Clopath, C. and Gerstner, W., Science **334**, p1569-1573 (2011).
[4] Butz, M. and van Ooyen, A. A Simple Rule for Dendritic Spine and Axonal Bouton Formation Can Account for Cortical Reorganization after Focal Retinal Lesions. PLoS Comput Biol; **9(10)**, (2013).

University of Hertfordshire UH

School of Engineering
and Computer Science

Poster Session

Brain-inspired spiking neural network for gas-based navigation

Rebecca Miko[1], Volker Steuber[1], and Michael Schmuker[1]
[1]Biocomputation Research Group, Center for Computer Science and Informatics Research, University of Hertfordshire

Introduction

The project aims to contribute towards solving gas-based navigation in robotics, using neural networks and processes similar to those found in mammalian brains. Odour stimuli in natural environments have a rich temporal structure that is caused by turbulent gas dispersion. It has been demonstrated that this structure contains information about the olfactory scene, for example the distance to an odour source [1,2]. Furthermore, it has been suggested that animals might exploit this structure and extract this information in order to locate odour sources [3]. Some of this information may lie in the temporal dynamics of the stimuli [2].

Event-based Coding

We analysed signals from data [4] which were collected in a wind tunnel using electronic gas sensors. The signal varies due to turbulence-induced fluctuations of gas concentration (Fig.1).

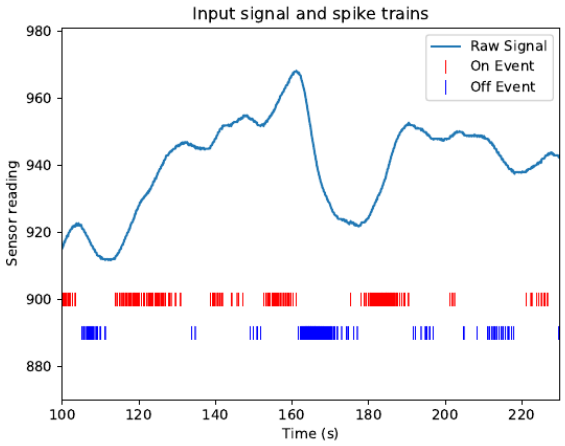

Figure 1: The output readings from the gas sensor data. We extracted ON and OFF events from the signal during periods where it is constantly rising (ON) or falling (OFF).

Source distance can be estimated from the number of "bouts" in the signal. A bout is a consistent change in the measured signal, for example a period where the concentration is constantly rising. The number of detected bouts increases with increasing source proximity [2].

We employ an event-based signal encoding paradigm that mimics computation in the brain, where neurons communicate via timed events, called spikes. To generate spikes from the gas signal, we first define a set of amplitude thresholds. A spike is generated each time the signal crosses a threshold. We used several sets of slightly different thresholds to create an asynchronous population code of spikes (Fig. 2). Asynchronous population codes are preferred because synchronous spiking could overload the connections between neurons. The "ON spikes" refer to bouts where the signal has increased and the "OFF spikes" are bouts where the signal decreased. The ON spike trains are fed into a network of Izhikevich neurons [5] as input. We investigate how a filter bank of bout detectors can infer information about odour proximity and guide gas-based navigation in robotics.

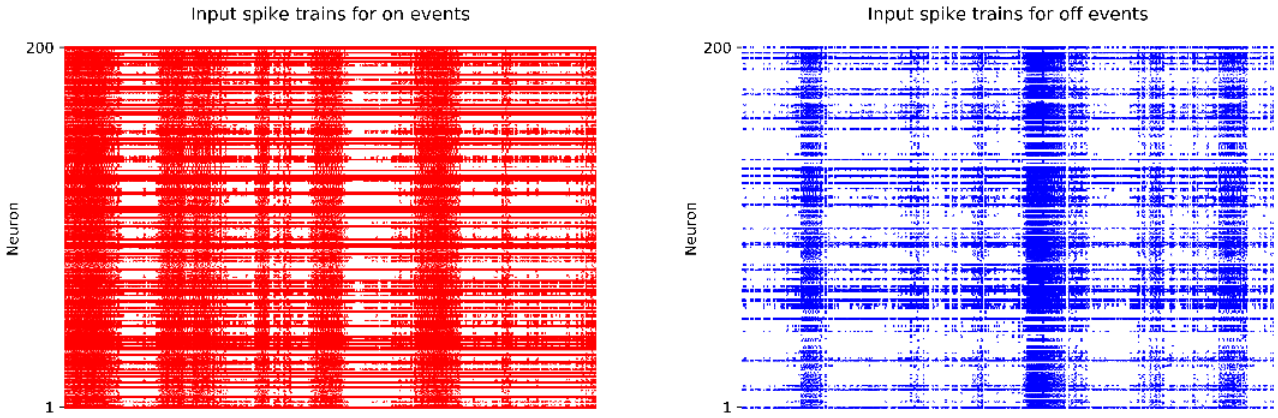

Figure 2: The raster plots show the input trains for 200 neurons when applying slightly different thresholds to the input signal. Left: the spike trains for ON events showing an overall increase in activity when the signal rises. Right: the OFF events showing an overall increase in activity when the signal falls.

Enose

We created an enose prototype to investigate whether we can determine bouts of odours using the method we applied to the network for event-based coding. The enose prototype has four metal oxide gas (MOX) sensors. They are mounted on an arduino where signals are read from the analog pins. The MOX sensors change resistance when binding with specific gases. This resistance change impacts the voltage read on the analog pins. The arduino then converts this analog signal into spikes and outputs events.

Enose Results

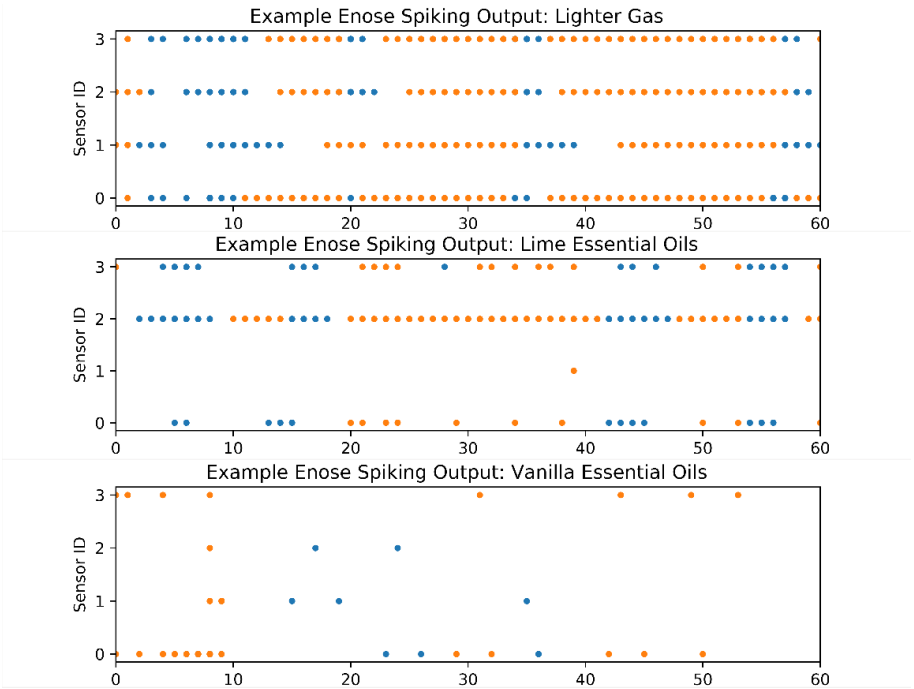

Figure 3: Examples of enose output using three different sources. The blue data points show ON events and the orange data points show OFF events. Upper panel: shows lighter gas causing the most activity for all four sensors. Center panel: shows the results from lime enssential oils, with little reaction from gas sensor 1. Bottom panel: shows the results from vanilla essential oils, demonstrating the least activity from all four sensors.

Conclusion

The results demonstrate that the enose has the ability to diffentiate between different odours. Additionally, the enose enables us to determine bouts of odours when using the same methods demonstrated in the event-based coding. With the ability to detect bouts, we take the first step towards calculating bout intervals and eventually infer distance to the odour source [2].

References

[1] Celani, A., Villermaux, E. and Vergassola, M.: Odor landscapes in turbulent environments. Physical Review X, 4(4), p.041015, 2014.
[2] Schmuker, M., Bahr, V. and Huerta, R.: Exploiting plume structure to decode gas source distance using metal-oxide gas sensors. Sensors and Actuators B: Chemical, 235, pp.636-646, 2016.
[3] Jacob, V., Monsempès, C., Rospars, J.P., Masson, J.B. and Lucas, P.: Olfactory coding in the turbulent realm. PLoS Computational Biology, 13(12), p.e1005870, 2017.
[4] Vergara, A., Fonollosa, J., Mahiques, J., Trincavelli, M., Rulkov, N. and Huerta, R., 2013. On the performance of gas sensor arrays in open sampling systems using Inhibitory Support Vector Machines. Sensors and Actuators B: Chemical, 185, pp.462-477.
[5] Izhikevich E.M. (2003), Simple model of spiking neurons, IEEE Transactions On Neural Networks, 14:1569-1572

A scale-up of processing non-woven flax tape and triaxial glass fibre composites

Gilles Toffe[1], Guogang Ren[1] *, Diogo Montalvão[2]

[1]University of Hertfordshire, School of Engineering and Computer Science, Hatfield, UK
[2]Bornemouth University, Bournemouth, UK

Abstract

In the drive towards a sustainable bio-economy, a growing interest in the development of composite materials using renewable raw resources is flourishing. One of these composites under our investigation has been flax fibre reinforced polylactic acid (PLA), known as a flax-tape composite (FTC). In this study, the manufacturing process of the flax tape and triaxial glass fibre fabric productions were evaluated through their life cycle assessment (LCA) using a gate-to-gate methodology of an input-output model, to estimate their energy demand and environmental impacts. The results showed that when the flax and PLA were mingled to produce a composite material in the form of a flax tape, the energy consumption was 0.25 MJ/kg, lower than 0.8 MJ/kg of triaxial glass fibre fabric composites.

1. Introduction

LCA takes a comprehensive gate-to-gate approach, thus focusing on only specific life cycle stage in material production and evaluation on the energy consumption, based on the recent series of ISO standards 14040 to 14043 provided in detailed guidelines for conducting LCA[1]. The attractiveness of natural fibres, as reinforcing materials, comes from their high specific strength, degradable property and low cost low-cost [2]. Therefore, natural fibres, such as flax and matrices polylactic acid (PLA) have witnessed a noticeable increase in sales volume, since they are rapidly penetrating European and Asian markets in building services, transportation (automotive, aerospace and marine/naval) and furniture [3-5]. However, synthetic fibre manufacturing has negative environmental impacts during its cradle-to-grave and gate-to-gate life cycle [6].To design and fabricate a new natural composite with a lower environmental footprint, compared to the synthetic composite material, some novel natural fibres are being considered to be the base of the matrix materials, for example, flax/PLA. Importantly, this work explored a relationship between the blending process and energy consumption of the flax tape composite in comparison to glass fibre composite, using a standard LCA analytical methodology.

2. Materials and methods

The methodology for modelling energy consumption and carbon dioxide demand was based on a study for machine tape in Tilsatec and triaxial glass fibre machine in Formax based in the UK. Tilsatec used purchase flax and PLA fibre in Europe (Belgium and France) for the production of composite flax tape. Formax used to purchase glass fibre tow to transform triaxial glass fibre in to the fabric. LCA Simapro 8.2 and ecoivent was used to measure and produce some of the primary and secondary data. The model of this study was constructed using SIMAPRO 8, a commercial LCA software product to produce the process tree and environment impact using weighting values to translate an inventory into a potential impact

on the environment. The measurement consists of using a domestic electricity usage monitor to compile gate-to-gate (GtG) LCA data for the project. A current sensor is clipped on to the supply cables on the machine connected to the transmitter, which then wirelessly sends real-time data to the energy monitor. The monitor receives the data and displays the demand in kilowatts of energy consumed at any given time. Therefore, the manufacturing process and energy consumption are input through the LCA SimaPro software 8 to be analysed.

3. Results and Discussion

The water emissions of nitrates, phosphates and nitrogen oxide (N0x) to air are higher as a result of fertiliser applications in natural fibre. The environmental impacts for the natural fibre composite are dominated by the energy and emissions from epoxy productions. Even though natural fibre accounts for 66% of the volume of the component, it contributes only 5.3 % of the cumulative energy demand[7]. As far as the energy demand, environmental impact load, water requirement consumption and solid waste are concerned, the flax/PLA composites have environmental advantages over their counterparts. This investigation provides useful information to the manufacturing, processors, consumers and policymakers of sustainable composites materials using flax tape. However, the LCA gate-to-gate can only be one of the references for the manufacturers and decision makers, since the weighting factors for different environmental impact on figure a and b categories depends on subjective expert opinion. On the other side, the gate-to-gate assessment of the flax tape does not include the product use and end-of-life phases, which limits the ability to identify the burden shifting.

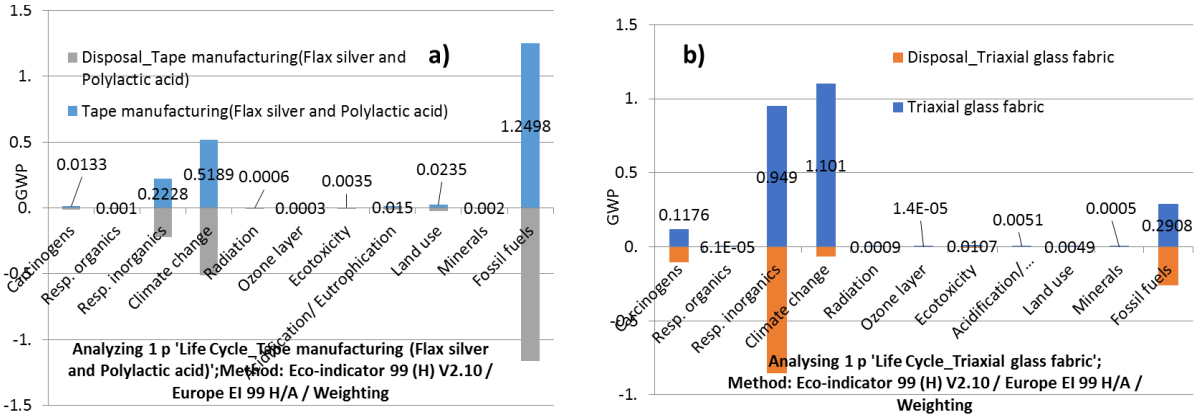

Figure a) and b): Show the environment impact of composite flax tape and triaxial glass fabric with SimaPro 8 software simulation.

The environmental impact of these materials has been investigated and calculated. The natural fibre composite material (Flax/PLA) has fewer processing steps to transform into the tape, therefore, consuming less energy and producing lower carbon dioxide emissions when compared to the synthetic glass fibre. The results obtained show that PLA commingled well with flax, as a matrix material for natural fibre composite. The energy consumption is estimated at 0.25 MJ/kg for the production of flax tape and 0.8 MJ/kg for triaxial glass fibre fabrics. Therefore, the production of composite flax tape uses lesser energy than some materials already being used in the industry.

4. Conclusions

It was clear that boundary selection had a significant influence on the gate-to-gate observed results. In this study, the manufacturing requirements to use flax, PLA and glass fibre input to produce composite materials with flax tape and triaxial glass fibre use purchased electric. The repercussions of comparing natural fibre to synthetic fibre could lead to significantly flawed conclusions. Hence, future research should focus on achieving equivalent or superior technical performance and component life.

References

1. ISO, I., 14040: Environmental management–life cycle assessment–principles and framework. London: British Standards Institution, 2006.
2. Pickering, K.L., M.A. Efendy, and T.M. Le, A review of recent developments in natural fibre composites and their mechanical performance. Composites Part A: Applied Science and Manufacturing. 83: p. 98-112.,2016.
3. RAJENDRAN, S., et al., Review of life cycle assessment on polyolefins and related materials. Plastics, rubber and composites. 41(4-5): p. 159-168.,2012.
4. Nyambo, C., A.K. Mohanty, and M. Misra, Polylactide-based renewable green composites from agricultural residues and their hybrids. Biomacromolecules. 11(6): p. 1654-1660.,2010.
5. Huda, M., et al., Wood-fiber-reinforced poly (lactic acid) composites: evaluation of the physicomechanical and morphological properties. Journal of Applied Polymer Science, 102(5): p. 4856-4869.,2006.
6. Pickering, K.L., et al., Influence of loading rate, alkali fibre treatment and crystallinity on fracture toughness of random short hemp fibre reinforced polylactide bio-composites. Composites Part A: Applied Science and Manufacturing, 42(9): p. 1148-1156.,2011.
7. X. Lu, M.Q.Z., M. Z Rong, D. L. Yue, G. C. Yang, Environmental degradability of self-reinforced composites made from sisal. Composites Science and Technology;64:1301-1310., 2014.

Investigating the Effects of Tooling Materials, Drill Geometry and Process Parameters on Hole Quality of Flax FRP Composite Laminate

Sikiru Oluwarotimi Ismail[1*], James Newman[1], Hom Nath Dhakal[2], and Funlade Sunmola[1]

[1]School of Engineering and Computer Science, University of Hertfordshire, Hatfield, Hertfordshire, AL10 9AB, England, United Kingdom
[2]School of Mechanical and Design Engineering, University of Portsmouth, Portsmouth, Hamsphire, PO1 3DJ, England, United Kingdom
*corresponding author: s.ismail3@herts.ac.uk

Abstract

Among natural fibre-reinforced polymer (FRP) composites, flax has an outstanding inherent properties. Holes are very important in both manufacturing and assembly of components. Hence, this study investigated the influence of tooling materials, drill geometry and process parameters on hole quality of 6 layers and vacuum bagging fabricated flax FRP/epoxy composite laminate, using L_{12} orthogonal array of Taguchi method. From the results obtained, it was evident that a combination of a lower feed rate, higher cutting speed with a bigger 13 mm coated HSS drill bit exhibited an optimal result/best hole quality. Therefore, they are recommended design specifications for drilling process of the flax FRP composite.

Keywords: Tooling materials; drill geometry; process parameters; hole quality; flax FRP composite laminate

Introduction

Advancement in materials design, development and process optimisation is an important driving force behind cutting-edge manufacturing technology. Fibre-reinforced polymer (FRP) composite laminate is one of the leading engineering materials. The outstanding inherent properties and significant applications of flax FRP composite laminate have attracted great attention of many sectors recently, among other natural FRP composites and importantly, when compared with synthetic counterparts [1]. These properties include, but are limited to, sustainability, renewability, biodegradability, ease and lower cost of production, lightweighting, environmental superiority, higher specific strength and stiffness as well as chemical, thermal, high corrosion and wear resistance [2]. Some of the major industries where FRP composites are increasingly used include transportation, telecommunication, construction, defence, power and games/sports. Moreover, drilling process during materials manufacturing is often necessary, as holes are required for coupling and/or assembling of components of many systems [2, 3]. Also, the quality of these holes depends on the correct selection of drill materials, geometry and drilling parameters, among other factors. Therefore, this study presents the effects of tooling materials, drill geometry and process parameters on hole quality of natural flax FRP composite laminate.

Experimental

The material sample was natural flax FRP epoxy-based composite laminate, fabricated by vacuum bagging technique and contained 6 layers or plies in ±45° orientation, as shown in Figure 1(c). It has a dimension of 231 x 231 x 6.44 mm. The tooling materials used were carbide, coated and uncoated HSS drill bits, as depicted in Figure 1 (a). Each of these types of drill bits has geometry (diameters) of 8 and

13 mm. After preliminary tests and based on past experience, the following process parameters were selected/used: cutting speeds of 40 and 80 mm/min and feed rates of 0.1 and 0.3 mm/rev, as lower and higher parameters. The drilling experiment was conducted on I020 VMC CNC drilling machine centre, as shown in Figure 1(b), using L_{12} orthogonal array of Taguchi method of design of experiment for feed rate and cutting speed to produce the spindle revolution in a dry environment/condition. The drilling-induced damage against the quality of the drilled holes was characterised using visual inspection, optical microscope and overall damage severity scores (ranking system). The results obtained are subsequently discussed.

Results and discussion

The results obtained depict that damage (uncut fibre and fibre fraying) increased with an increase in feed rate, but reduced with an increase in cutting speed. These were more prominent with drill bit of smaller diameter, as depicted in Figure 1(d). The coated HSS drill performed best, followed by carbide and uncoated performed worst. The best quality holes were obtained in a best combination of 13 mm coated HSS, with the higher cutting speed and lower feed rate, as similarly reported [3, 4]. However, the worst holes were obtained with 8 mm uncoated HSS drill bit, using the lower cutting speed and feed rate. These damage responses could be attributed to the advantageous effects of coating on HSS drill bit, higher cutting speed, lower feed rate [3] and bigger drill diameter on developed cutting forces (thrust and torque) and interfacial heat transfer rate during drilling phenomenon. In addition, it was evident that a higher cutting speed led to an increase in the amount of fibre fraying that occurred, but it reduced the amount of uncut fibres that were present after drilling process. Summarily, the higher cutting speed led to a lower level of overall damage, as visually and microscopically examined, and using damage (fibre fraying and uncut) severity scores.

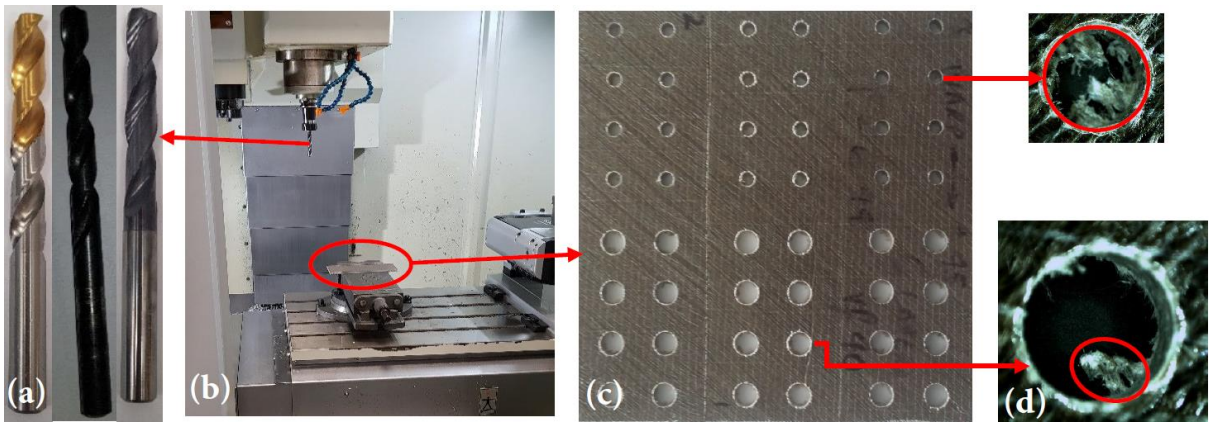

Figure 1. (a) A set of 8 mm coated, uncoated HSS and carbide drills used, (b) experimental set-up, showing positions of both drill and flax FRP composite on I020 VMC drilling machine, (c) drilled flax FRP composite sample and (d) microscopic damage responses

Conclusion

The effects of tooling materials, drill geometry and process parameters on hole quality of flax FRP composite laminate have been investigated. When designing for the manufacturing process of drilling this flax FRP/epoxy composite, a lower feed rate, higher cutting speed with a 13 mm coated HSS drill bit (optimum results) are evidently required. Comparative study on similar natural fibres, such as hemp, jute, abaca FRP composites, among others is recommended for future work as well as further characterisation of damage responses, such as surface roughness and delamination.

Reference

[1] H. N. Dhakal et al. *The international Journal of Advanced Manufacturing Technology* **99**, 2933. (2018).
[2] D. Wang et al. *Composites Part A: Applied Science and Manufacturing* **119,** 188. (2019).
[3] S. O. Ismail et al. *Proceeding of IMechE Part B: Journal of Engineering Manufacture* **231**, 2527. (2017).
[4] S.O. Ismail et al. *Engineering Science and Technology, an International Journal* **19,** 2051. (2016).

Using Feature Weighting as a Tool for Clustering Application

Deepak Panday[1*], Peter Lane[2], and Na Halen[3]
[1,2,3]*University of Hertfordshire*
d.panday@herts.ac.uk

In this research, we explore two areas of data pre-processing: feature selection and imputation of missing values. We have used feature weighting technique to address these issues in synthetic datasets from mixed-model Gaussian distribution. Our experiments show that using feature weight for feature selection results better cluster recovery. Throughout the experiments, we have also found out that the regression-based imputation methods have higher cluster recovery in weighted variates of kMeans.

Keywords: feature weighting; Gaussian mixed-model; feature selection; missing values; validation index.

Introduction

Clustering provides a fundamental base for exploratory data mining and has been exploited in many applications. Features so far have been treated equally in most research, regardless of their actual degree of relevance to the nature of a given dataset. Feature weighting, which assigns a weight to each feature- the greater the value the more salient the feature, was proposed by Huang et. al.[1]. This research is focused on weighting in two clustering applications:

A. Using feature weighting as a tool for feature selection
   For feature selections two algorithms- Feature Selection via mean Feature Weighting (meanFSFW) and Feature Selection via max Feature Weighting (maxFSFW)[2] were developed based on the feature weighting techniques.
B. Addressing missing values in the weighted variant of kMeans.
   In the case of missing values, we observed the best possible imputation methods to replace the missing values in weighted kMeans (wKMeans) and intelligent weighted kMeans (iWKMeans).

Experiments

For experiments, we generated four sets of datasets (100x8, 100x12, 100x16, and 100x20) from mixed model Gaussian distribution as shown in Table 1. Each of these datasets consists of 1000 entities. The number of Gaussian components of each of these components are 2, 3, 4 and 5 respectively. In addition, various numbers of noise features are added to the original datasets.

			Features		
Data set	Entities (n)	Clusters (K)	Original	Noise	Total (m)
1000x8-2	1000	2	8	0	8
1000x8-2 + 4NF	1000	2	8	4	12
1000x8-2 + 8NF	1000	2	8	8	16
1000x12-3	1000	3	12	0	12
1000x12-3 + 6NF	1000	3	12	6	18
1000x12-3 + 12NF	1000	3	12	12	24
1000x16-4+8NF	1000	4	16	0	16
1000x16-4	1000	4	16	8	24
1000x16-4+16NF	1000	4	16	16	32
1000x20-5	1000	5	20	0	20
1000x20-5+10NF	1000	5	20	10	30
1000x20-5+20NF	1000	5	20	20	40

Table1. Synthetic datasets generated from mixed-model Gaussian distribution

In the case of feature selection, we assumed that a noisy feature had a uniform distribution. These features have higher dispersion compared with the original features, and hence have low feature weights. In meanFSFW, the mean of the cluster-based feature weights was chosen, and in the maxFSFW, the maximum of cluster-based feature weights was chosen as feature weight. Both versions of FSFW removed features less than 1/m (where m is the total number of features). For the second

experiments, various type of noise were inserted into the datasets as missing values. These missing values had univariate missing pattern and missing completely at random (MCA) missing mechanism.

Results and discussion

Adjusted recovery index (ARI) was used to measure the performance of the algorithms in both experiments. Best result along a row is bold in the tables below.

		FS using Feature Similarity		Multi-Cluster FS		FS using Feature Weight	
Data sets	*k*-means	SIL	Best Case	SIL	Best Case	meanFSFW	maxFSFW
1000x8-2	**0.965/0.04**	0.935/0.08	0.937/0.08	0.958/0.06	0.958/0.06	0.932/0.10	0.898/0.13
1000x8-2 +4NF	0.788/0.39	0.772/0.39	0.920/0.13	0.789/0.39	0.891/0.25	**0.965/0.05**	0.818/0.36
1000x8-2 +8NF	0.768/0.40	0.771/0.39	0.922/0.12	0.770/0.41	0.847/0.32	**0.965/0.05**	0.859/0.32
1000x12-3	**0.984/0.03**	0.973/0.04	0.974/0.04	0.983/0.03	0.984/0.03	0.949/0.09	0.915/0.14
1000x12-3 +6NF	0.930/0.19	0.917/0.19	0.963/0.07	0.930/0.19	0.937/0.18	**0.983/0.03**	0.947/0.16
1000x12-3 +12NF	0.915/0.20	0.917/0.19	0.964/0.06	0.926/0.19	0.934/0.18	**0.984/0.03**	0.958/0.13
1000x16-4	**0.996/0.01**	0.993/0.01	0.993/0.01	0.995/0.01	0.996/0.0	0.977/0.03	0.946/0.07
1000x16-4 +8NF	0.987/0.04	0.977/0.07	0.988/0.02	0.987/0.05	0.989/0.05	**0.996/0.01**	0.991/0.01
1000x16-4 +16NF	0.985/0.04	0.973/0.07	0.986/0.02	0.985/0.05	0.987/0.05	**0.996/0.01**	0.994/0.01
1000x20-5	0.998/0.02	0.997/0.01	0.997/0.01	**0.999/0.00**	0.999/0.00	0.991/0.01	0.976/0.03
1000x20-5 +10NF	0.992/0.03	0.995/0.01	0.996/0.01	0.994/0.03	0.994/0.03	**0.999/0.00**	0.996/0.01
1000x20-5 +20NF	0.988/0.04	0.994/0.01	0.995/0.01	0.994/0.02	0.995/0.02	**0.999/0.00**	**0.999/0.00**

Table2. Comparison of different feature selection algorithms based on adjusted random index (ARI).

The first column Table 2 represents the databset and the remining columns read the adjusted rand index (ARI) from different algorithms. The first algorithm, kMeans was fed datasets without feature selection and was considered as a benchmark. Both feature selection using feature similarity, FSFS [3] and multi-cluster base feature selection, MCFS [4] required number of features selected to be known. Silhouette index was used to turn the parameter in both algorithms. The base case results for these algorithms represent the best case without parameter tuning.

	WKMeans				Intelligent WKMeans			
DataSet	F Avg	KNN	S Regression	C Regression	F Avg	KNN	S Regression	C Regression
1000x8	**0.971/0.04**	**0.971/0.04**	**0.971/0.04**	**0.971/0.04**	**0.197/0.06**	0.196/0.05	0.195/0.05	0.195/0.05
1000x12	**0.922/0.18**	**0.922/0.18**	**0.922/0.18**	**0.922/0.18**	0.372/0.13	0.377/0.13	0.376/0.13	**0.378/0.13**
1000x16	**0.881/0.17**	**0.881/0.17**	**0.881/0.17**	**0.881/0.17**	0.624/0.12	**0.625/0.12**	0.624/0.12	**0.625/0.12**
1000x20	**0.856/0.15**	**0.856/0.15**	**0.856/0.15**	0.855/0.15	**0.85/0.09**	0.849/0.09	0.849/0.09	0.848/0.09

Table3. Observation of different imputation methods for weighted kMeans and intelligent weighted KMeans.

The first column in Table 3 represents dataset configuration. The remaining columns contain ARI values from two sets of experiments: weighted KMeans (wKMeans) and intelligent WKMeans. For each set, we have four different imputation methods: feature average imputation, KNN imputation, simple regression-base imputation and cluster-based regression imputation were used impute missing values.

Conclusion

Both meanFSFW and maxFSFW outperform two of the most popular feature selection algorithms: Feature Selection using Feature Similarity and Multi-cluster Feature Selection. In most of the cases, regression-based imputation had outperformed other imputation methods. For future work, this research can be extended to real-world datasets.

Reference

1. Joshua Zhexue Huang, Michael K Ng, Hongqiang Rong, and Zichen Li. Automated variable weighting in k-means type clustering. IEEE Transactions on Pattern Analysis and Machine Intelligence, 27(5):657-668, 2005.
2. Panday, D., Amorim, R.C., Lane, P., Feature weighting as a tool for unsupervised feature selection. Information Processing Letters, Elsevier, vol. 129, pp. 44-52, 2018.

3. P. Mitra, C. Murthy, S. K. Pal, Unsupervised feature selection using feature similarity, Pattern Analysis and Machine Intelligence, IEEE Transactions on 24 (3) (2002) 301–312.
4. D. Cai, C. Zhang, X. He, Unsupervised feature selection for multi-cluster data, in: Proceedings of the 16th ACM SIGKDD international conference on Knowledge discovery and data mining, ACM, 2010, pp. 333–342

Modal Parameters Response to Increased Energy Absorption in CFRP Laminates

Amafabia, Daerefa-a Mitsheal[1], David-West, Opukuro [1], Montalvão, Diogo [2], and Haritos, George[3]

[1] Division of Automotive, Mechanical and Mechatronics Engineering, School of Engineering and Technology, University of Hertfordshire, Hatfield AL10 9AB, United Kingdom.

[2] Department of Design and Engineering, Faculty of Science and Technology, Bournemouth University, Poole House, Talbot Campus, Fern Barrow, Poole BH12 5BB, United Kingdom.

[3]School of Engineering and the Environment, Kingston University London, Kingston upon Thames, Penrhyn Road KT1 2EE, United Kingdom.

*corresponding author: d.amafabia@herts.ac.uk

Abstract: Although damage identification in CFRP composite structure using modal parameters has been ongoing for years, little has been done on studying the effect of energy increase on the modal parameters. In this work, three different energy levels; 5.5J, 12.6J and 16.6J were introduced to the test sample and the response of the global properties (modal frequency and modal damping) were monitored. The results show that unlike the modal damping, as the amount of energy absorbed increases, the modal frequency reduces further at most modes. It has an edge over modal damping in terms of damage detection in CFRP composite laminates.

Keywords: Laminates; Stacking sequence; Modal analysis; Frequency response functions; Modal frequency

1.0 Introduction

Composite materials have gained wide acceptance in industries such as aerospace, marine, automotive, civil infrastructures and sports equipment, due to their unique mechanical properties, namely strength and stiffness-to-weight ratios [1–5]. Composites result from the combination of two or more distinct materials to form a single material that has enhanced mechanical properties when compared to the individual properties of the constituent elements. In the particular case of composite laminates, these are composed of two or more layers that are laid up together [6], reinforced with aligned fibres [7] and a matrix, such as an epoxy resin, acting as a bonding medium. However, during maintenance, assembling, or in use, a composite material is often subjected to low-velocity impacts which result in BVID [3,8]. This is due to the deficiency in the through-thickness properties of the composite laminate [9]. The impact on the surface would not show many visible marks, but a noticeable mark on the opposite side of the material which is usually not accessible through visual inspection. That could compromise the integrity of the composite material and reduce its life cycle. Hence, this work is focused on studying the behaviour of both the modal frequency and modal damping as the energy absorbed in Carbon Fibre Reinforced Polymer (CFRP) increases.

2.0 Experiemental

In this study, CFRP laminates of different stacking sequence manufactured by hand lay-up and autoclave curing were used to conduct the free-free experimental modal analysis (EMA) within the frequency range of 0 -- 800 Hz. The specimens were suspended vertically as shown in Figure 1 a, under a free-free simulated configuration with 2 strings of nylon, which were attached to 1mm diameter at 50mm apart from the edge of the test plate and 5mm from its top edge. An electrodynamic shaker (LDS V406 M4-CE) with pushrod 60mm long connected to a force transducer, is used to start a single point excitation signal within the range of 0 to 800Hz with a 0.25 resolution that was generated and amplified using a NI 9263 analogue output module and an LDS PA25E power amplifier.

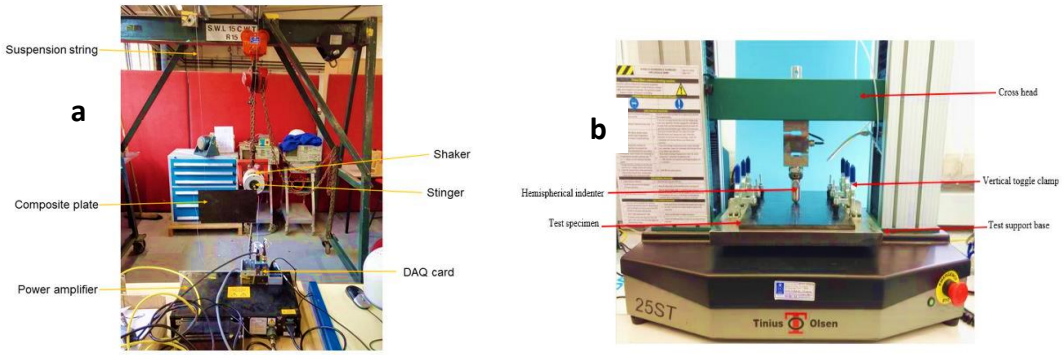

Figure 1 Experimental testing in the left (a) Vibration Testing, (b) Static testing

The responses were measured at a specific location using three lightweight PCB teardrop accelerometer, type 352A24, that weighs 0.8 g each, at the corner of the specimen to acquire the Frequency Response Functions (FRFs). The experiments were performed for both healthy and damage induced samples of the same configuration. The damage was introduced in the test sample through static testing (see Figure 1 b).

3.0 Results and discussion

The impact on the modal damping factors and natural frequencies were observed and the results presented as shown in Figure 2, which is a representative result of the study conducted. In the figure, there is a reduction in the modal frequencies from modes 2 to 4 after the absorbed energies were increased successively. While from modes 5 to 10 recorded an increase in the modal damping across all the three tests.

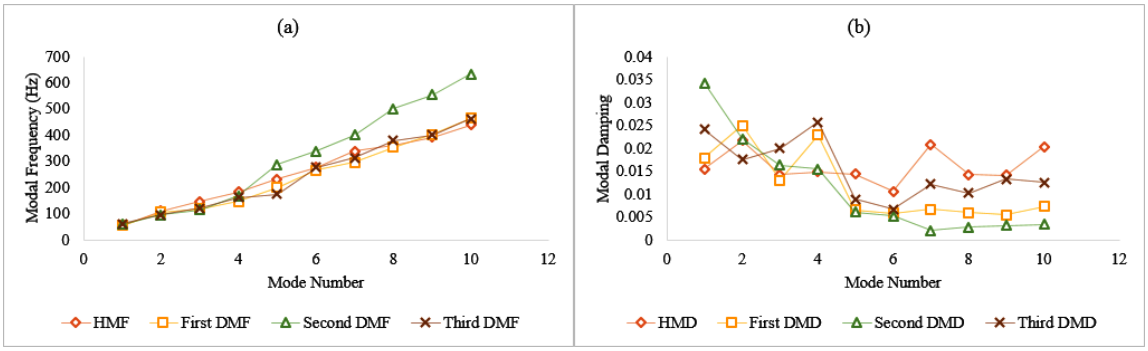

Figure 2 Modal parameters response to the increased energy level in plate A1: (a) Modal frequency (b) Modal damping

4.0 Conclusion

The importance of composite CFRP in several industries cannot be overemphasized. Although not at every mode the modal frequencies have indicated more capability than the modal damping, in identifying the damage locality in a CFRP laminate. From the result, it was observed that as the impact energy increases, both the modal frequency and modal damping responds differently at individual modes.

Reference

[1] Kessler SS, Spearing SM, Soutis C. Damage detection in composite materials using Lamb wave methods. Smart Mater Struct 2002;11:269–78.

[2] Ye Lin, Ye Lu, Zhongqing Su GM. Functionalized composite structures for new generation airframes: a review. Compos Sci Technol 2005;65:1436–46.

[3] Montalvão D, Ribeiro AMR, Duarte-Silva JAB. Experimental Assessment of a Modal-Based Multi-Parameter Method for Locating Damage in Composite Laminates. Exp Mech 2011;51:1473–88.

[4] Montalvão Diogo, Dimitris Karanatsis, António MR Ribeiro, Joana Arina RB. An experimental study on the evolution of modal

damping with damage in carbon fiber laminates. Ournal Compos Mater 2014;49:2403–13.
[5] Huang, L., Sheikh, A. H., Ng, C. T., Griffith MC. An efficient finite element model for buckling analysis of grid stiffened Laminated composite plates. Compos Struct 2015;122:41–50.
[6] Varga M, Vretenar V, Kotlar M, Skakalova V, Kromka A. Fabrication of free-standing pure carbon-based composite material with the combination of sp2-sp3 hybridizations. Appl Surf Sci 2014;308:211–5.
[7] Notta-Cuvier D, Lauro F, Bennani B, Balieu R. Damage of short-fibre reinforced materials with anisotropy induced by complex fibres orientations. Mech Mater 2014;68:193–206.
[8] Shyr T-W, Pan Y-H. Impact resistance and damage characteristics of composite laminates. Compos Struct 2003;62:193–203.
[9] Zhang J, Zhang X. Simulating low-velocity impact induced delamination in composites by a quasi-static load model with surface-based cohesive contact. Compos Struct 2015;125:51–7.

Improving Energy Disaggregation Performance Using Appliance-Driven Frame-Lengths

Pascal A. Schirmer* **and Iosif Mporas**
*corresponding author: p.schirmer@herts.ac.uk

This paper proposes a new appliance-driven selection of frame-lengths for improving the energy disaggregation in Non-Intrusive Load Monitoring (NILM). Specifically, the methodology uses a machine learning model with parallel binary device detectors and optimized device dependent frame-lengths in order to improve device identification. The performance of the proposed methodology was evaluated on a state-of-the-art baseline system across several publicly available datasets increasing performance up to 5.2% in terms of estimation accuracy when compared to the baseline system without device dependent frame-lengths.

Keywords: Non-Intrusive Load Monitoring (NILM), Energy Disaggregation, Device Classification, Frame-Lengths

Introduction

With the rising need of electrical energy and the increasing number of energy consuming devices the accurate and fine grained monitoring of electrical energy consumption within residential and industrial buildings has become a crucial issue [1]. Furthermore the establishment of smart grids, renewable energies and demand management [2] increases the need for real-time monitoring of both power generation and consumption [1], while the extensive gathering of information through smart-meters and the detection of detailed household energy information raises concerns regarding consumer privacy and energy data protection [3]. To address those challenges analysis of energy consumption on device level is necessary.

Proposed Architecture

The proposed methodology uses a two-stage classification scheme, with the first stage consisting of a set of *M* binary classifiers (device detectors) $\boldsymbol{b_i}$ processing the aggregated signal in parallel and each of them producing a device-specific detection score according to the optimal frame-length ***F()*** (i.e. a probability of existence of that device). The second stage consists of a regression model for detection of electrical appliances, which uses as input the scores produced at the first stage and estimates the power consumption per device. Since in real-world applications not all devices are apriori known, in this methodology we consider except of a closed-set of known devices also a ghost-power detector (i.e. the power consumption of one or more unknown devices). The block diagram of the proposed methodology is illustrated in Figure 1.

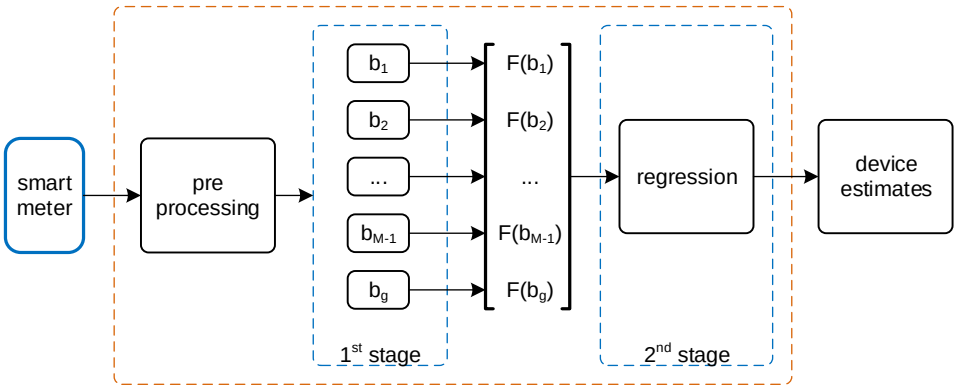

Figure 1. Proposed architecture with appliance-dependent frame-lengths for energy disaggregation.

Experimental Results and Discussion

The presented architecture was evaluated using five datasets of the *ECO* database [4]. The performance was evaluated in terms of estimation accuracy (E_{ACC}) considering device operation in state level with a double counting for errors, i.e.

$$E_{ACC} = 1 - \frac{\sum_{t=1}^{T}\sum_{m=1}^{M}|\hat{p}_t^m - p_t^m|}{2\sum_{t=1}^{T}\sum_{m=1}^{M}|p_t^m|} \quad (1)$$

where *T* is the number of frames, *M* the number of appliances and $\hat{p}_t^m$ the power estimate.

Table 1: Energy disaggregation performance for 5 different datasets out of the ECO database using different frame-lengths

Dataset	5	10	15	20	25	30	'Opt'
ECO-1	84.0%	81.2%	84.1%	**87.7%**	86.5%	81.5%	**91.4%**
ECO-2	86.4%	83.1%	80.7%	82.8%	**86.9%**	81.4%	**87.6%**
ECO-4	80.1%	79.8%	**82.3%**	79.4%	79.9%	78.1%	**83.5%**
ECO-5	83.9%	83.3%	81.0%	73.2%	**85.7%**	82.0%	**86.7%**
ECO-6	**72.3%**	71.3%	70.9%	69.4%	57.6%	61.3%	**77.5%**

The results in Table 1 show the significant effect of the frame-length on the disaggregation accuracy. Figure 2 shows two common electrical appliances, namely a washing machine (*WM*) and a fridge. As can be seen in Figure 2 the *WM* disaggregation accuracy improves from shorter frame lengths due to its stronger time varying power consumption pattern while the opposite is observed for the fridge.

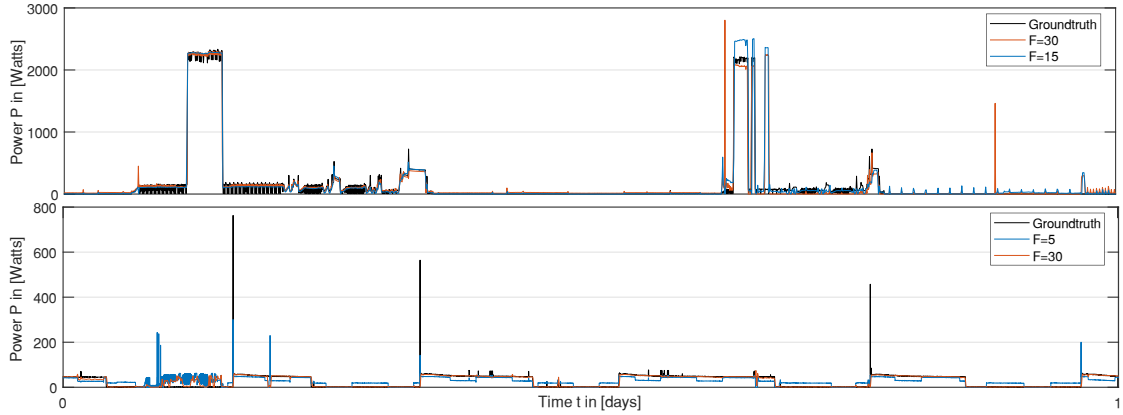

Figure 2. Active power consumption of a fridge and a washing machine including ground truth and disaggregated signals with two different frame lengths (fridge: F=5 (71.9%) and F=30 (93.3%) / WM: (F=15 (80.3%) and F=30 (71.2%))

Conclusion

A methodology for energy disaggregation using appliance-driven frame-lengths was presented. The methodology extends the baseline NILM approach using device-specific information. The maximum improvement in terms of absolute increase of estimation accuracy was equal to 5.2% and significant improvement was observed for devices with repetitive working routines.

Reference list

[1] Siddharth Bhela et al, "Enhancing observability in power distribution grids," in 2017 IEEE International Conference on Acoustics, Speech and Signal Processing, Piscataway, NJ, 2017, pp. 4551–4555, IEEE.
[2] Adriana Chis et al, "Demand response for renewable energy integration and load balancing in smart grid communities," in 2016 24th European Signal Processing Conference (EUSIPCO), Piscataway, NJ, 2016, pp. 1423–1427, IEEE.
[3] Zuxing Li et al, "Privacy- preserving energy flow control in smart grids," in 2016 IEEE International Conference on Acoustics, Speech, and Signal Processing, Piscataway, NJ and Piscataway, NJ, 2016, pp. 2194–2198, IEEE.
[4] Christian Beckel et al, "The eco data set and the performance of non-intrusive load monitoring algorithms," in BuildSys'14, Mani Srivastava, Ed., New York, 2014, pp. 80–89, ACM.

Measuring Habituation during Human-Robot Interaction

Grigorios D. Skaltsas
University of Hertfordshire

Using measurements of physiological signals (eye-tracking, galvanic skin response, heart rate) and questionnaires during a series of human-robot interaction experiments, user stress metrics and habituation patterns are analysed. The experimental results indicate that there seems to be a varying relation between human stress and robot speed as the human gets acquainted with the robot which seems to be also affected by the human perception of the task's success.

Introduction

Reading and evaluating the human's adaptation through biological signals could be the base for a performance optimization system targeting the minimization of human stress during the interaction [2-4]. It has been shown that safety is still perceived as low when the robot's trajectory planning and execution seems to be only avoiding collision [1].

For the purpose of this study, the following signals were chosen to be analyzed in combination:

1) Galvanic Skin Response (GSR) consists in reading the changes in human skin's conductivity when the sweat micro-glands respond to stressful situations.
2) Eye-Tracking (ET) offers physiological and subjective evaluation by correlating ET data with questionnaire responses.
3) Heart Rate (HR) Heart-rate in HRI has been used as a primary physiological response measure.

Additionally, questionnaires were designed to help humans reflect on their experience and the data resulted is combined with the methods mentioned above. As a user feedback method, questionnaires have been widely used in HRI [1].

The objectives are: Compare the findings of previous experiments in related studies verifying that the results are similar [5, 6, 7]. Provide actual data on HRI sessions, where the human is passively participating, both from questionnaires and sensor readings. Explore the habituation patterns that might appear, create the proposed statistical model as a correlation between the sensor readings and the replies on the questionnaires.

Experimental

The experiment explored short-term habituation and had participants mostly being students and local residents from the nearby area that can access the university easily. The sample contained 29 participants (Male: 22, (Age: 34.5avg 10.7std) Female: 5 (28avg 4.9std)). Their knowledge on digital equipment was marked high on the average. The participants were split in four groups. All groups had to experience four distinct sessions. For the habituation effects' study, all the sessions run sequentially with a small pause in between for a few minutes until the questionnaires are completed. The users had to evaluate their experience with the robot, combining it with the overall effectiveness of the task, whilst their physiological responses were recorded. After the participants entered the lab, they read the participant information sheet and signed the consent form, the sensors were then fitted, calibrated and tested on each user on an individual basis at the beginning of the experiment. In order to obtain a base line for the GSR, a small resting period was introduced. The ET sensor had to be calibrated on an individual basis. To keep the base GSR updated, small pauses of a minute were introduced between the completion of the questionnaire and the next session. In each session, the robot approached them from a distance of approximately 5 meters after coming out of an initial location where it would not be visible to the user. The robot during each session acted in a fully autonomous way, acting totally independent of any of the user's sensor measured feedback. The

structure of the sessions was based on the combination of two conditions. The first condition was the robot's speed and hence the perceived risk by the human of the robot crashing onto a wall or on the human upon approach. The speed choices were based on the robot's capabilities. The second was the delivery of an item that was on the robot but not securely attached to it, hence an extra risk perceived by the human as task failure, such as dropping the item at some point or seeing the item shaking during the transportation. For this experiment, the item chosen was a half full semitransparent water bottle. The user could see the shake of the water during its transportation by the robot. These conditions result in the following session scenarios: Fast/slow slow carrying the bottle, fast/slow without carrying the bottle.

To avoid bias, users were grouped as described earlier and set to participate in possible combinations of sequences of session scenarios as shown on table 1. The first two sessions for each group consist of the robot varying its speed alone. The last two sessions add the bottle carrying task combined with the variations of the speed. Adding the extra risk at the last two sessions of the experiment, compensates for the user's loss of interest and changing one condition each time helps compare the changes in the habituation pattern of each group in a controlled manner.

The robot did not communicate to the user its movement intentions in any session. The users experienced the robot planning its movement spontaneously from by their visual perception of the robot's location and the engine's noise via the custom platform "sunflower". It is a service robot comprising of a mobile base, a waist link, and a tray (http://lirec.eu/project). It is a medium sized robot built on a Pioneer 3DX base.

The path of the robot (figure 1) was chosen with a maneuver that requires a sharp turn (top right corner) and the potential of a crash upon failure when it was still away from the user. The duration is 48 seconds for the slow and 20 seconds for the fast session, giving enough time to the user's GSR to rise or fall.

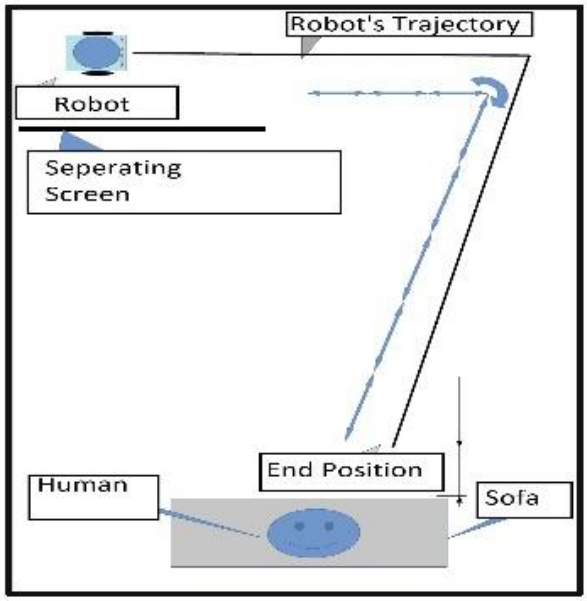

Figure 1. Robot's trajectory

There are four questionnaires used for this experiment. The (1) "demographics sheet" asking age, gender, expertise with computers among others, the (2) "behind the wall" asking about the users experience whilst the robot was not visible and one copy of the (3) "main questionnaire" was handed out to the user whilst the sensors were still fitted. The (3) "main questionnaire" was handed to the

user after each trial. Hence it was completed four times for each user. It asked the user to evaluate the robot's performance. It also required the user to indicate on a schematic showing the robot's trajectory during the trial, the parts where the robot was too fast or slow as well as where it could have failed the task. The (4) "general questionnaire" -which is handed out in the end- asking the user about his/her overall experience, as well as the (4) "demographics sheet" have the purpose to normalise the responses of the user. In a similar fashion, a second experiment took place at Technical University of Vienna, Austria. The platform used was PEPER (softbank.com).

Results and discussion

From a qualitative point of view, there seem to be repeated patterns for most users' physiological responses in relation to specific events. User perception of the task's risks and complexity varies seemingly as the conditions vary in ways that the physiological responses do not always correspond to the questionnaire responses.

Emerging features such as stress signs due to specific event anticipation and their variance are currently being studied. For example, once the user has experienced the robot's trajectory for the first time, how long it takes before the turning point is reached and hence his/her GSR peaks anticipating the potential crash on the wall.

Reference list

[1] P. A. Lasota, T. Fong, J. A. Shah, and others, "A survey of methods for safe human-robot interaction," *Foundations and Trends in Robotics,* vol. 5, no. 4, pp. 261-349, 2017.

[2] R. R. Fletcher, K. i. Amemori, M. Goodwin, and A. M. Graybiel, "Wearable wireless sensor platform for studying autonomic activity and social behavior in non-human primates," in *Proc. Annual Int. Conf. of the IEEE Engineering in Medicine and Biology Society*, 2012, pp. 4046-4049.

[3] I. Daly *et al.*, "Towards human-computer music interaction: Evaluation of an affectively-driven music generator via galvanic skin response measures," in *Proc. 7th Computer Science and Electronic Engineering Conf. (CEEC)*, 2015, pp. 87-92.

[4] A. Sano and R. W. Picard, "Stress Recognition Using Wearable Sensors and Mobile Phones," in *Proc. Humaine Association Conf. Affective Computing and Intelligent Interaction*, 2013, pp. 671-676.

[5] F. Dehais, E. A. Sisbot, R. Alami, and M. Causse, "Physiological and subjective evaluation of a human-robot object hand-over task," *Applied ergonomics,* vol. 42, no. 6, pp. 785-791, 2011.

[6] T. Arai, R. Kato, and M. Fujita, "Assessment of operator stress induced by robot collaboration in assembly," *CIRP annals,* vol. 59, no. 1, pp. 5-8, 2010.

[7] D. Kulic and E. Croft, "Anxiety detection during human-robot interaction," presented at the Intelligent Robots and Systems, 2005.(IROS 2005). 2005 IEEE/RSJ International Conference on, 2005.

[8] lirec.eu. Available: http://lirec.eu/project

Politics and Power in Software Requirements Engineering

Rana Siadati, Catherine Menon, Paul Wernick, and Vito Veneziano
University of Hertfordshire, School of Engineering and Computer Science, Department of Computer Science

Context and Objectives

This research study focuses on how politics and power relationships can (and unfortunately usually does) affect in a negative way the outcome of any software requirements engineering exercise within any organization, and it aims at enabling practitioners (requirements engineers, system analysts, software engineers) at capturing, modelling and somehow managing politics within that organization.

Background

Traditionally, politics and power have been seen as secondary factors, well below the technical component of the requirements engineer's role, notwithstanding the fact that most of large software projects fail for non-technical reasons (as reported by [1],[2]). This has meant that over-simplified views and considerations of such aspects have become predominant in how we train requirements engineers: such views may well have contributed to a selective blindness for power dynamics and how they do not always propagate linearly, from top to bottom, but rather follow more complex patterns. Likewise, the adoption across the field of notations and technical language(s) from engineering (e.g., organigrams and UML) with limited ability to express, for example, ambiguity, to represent complex phenomena like organisations, can result in models that only capture a static, structural view, as if complex, changing webs of personal relationships in an organisation can be the object of just another engineering blueprint. This has in our opinion led to an implicit decision to ignore or abstract away how organisations become permeated by political relationships in a fluid, dynamic and sometimes unpredictable way.

Methodology

For this reason, we are now working towards a simple notational tool designed for requirements engineers and aimed at capturing politics and power relationships within organisations. This tool has been intentionally designed to be simple and fast to use in conjunction with (and "augmenting") the traditional repository of more traditional, technically-focused modelling techniques used by practitioners for capturing and specifying requirements.
Its value would be assessed by means of the impact evaluation methodology, a type of counterfactual evaluation analysis with an arising consensus [3], well established in policy-making and politics-related fields.

Results and conclusions

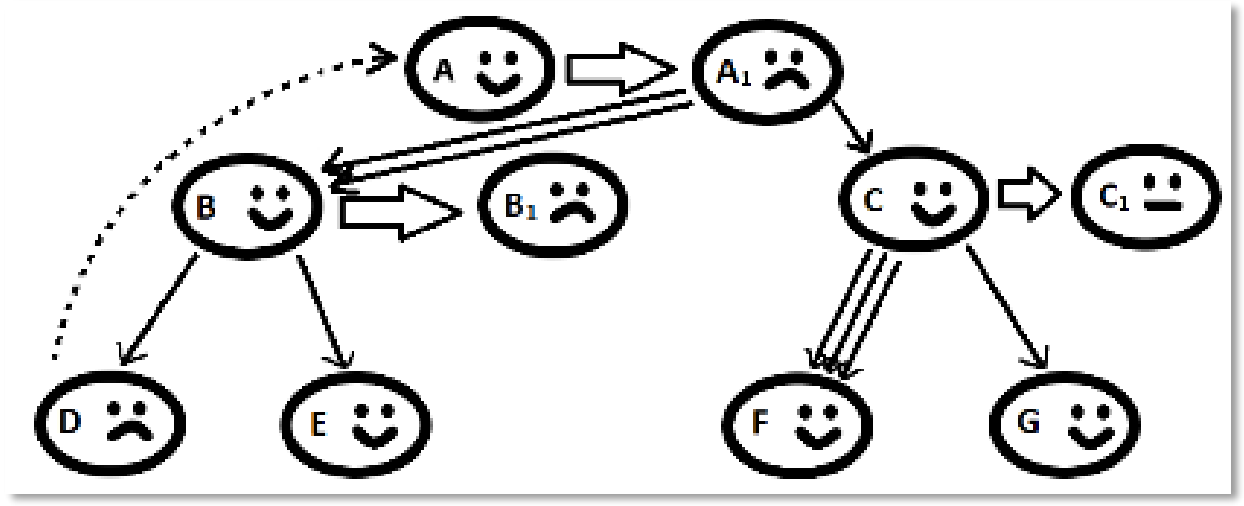

Figure 1: Example of notation representing dynamics of informal influences within an organization against a certain requirement

An applied example of this notation, representing informal influences affecting decision makers and stakeholders within an organization, is included in the Figure 1.

The suggested graphical notation for modelling the political context in RE would maybe not solve the problem: but even if it just raises awareness, this would make us closer to solving the problem.

References

[1] Geethalakshmi, S.N. and Shanmugam A. (2008), Success and Failure of Software Development: Practitioners' Perspective. Proceedings of the International Multi Conference of Engineers and Computer Scientists 2008, Vol I IMECS 2008, 19-21 March, 2008, Hong Kong.

[2] Hull E., Jackson K. and Dick J. (2002), Requirements Engineering. Springer, Cham.

[3] White, H. (2009) Theory-based impact evaluation: Principles and practice, Working Paper 3, International Initiative for Impact Evaluation, New Delhi

Searching for Asynchronous Irregular Activity in Balanced Real-Time Spiking Neural Networks: Reproducing a Parameter Search using Neuromorphic Hardware

Samuel Sutton [1*], Volker Steuber [1], and Michael Schmuker [1]
[1]*Biocomputation Research Group, Centre for Computer Science and Informatics Research, University of Hertfordshire*
*corresponding author: s.sutton3@herts.ac.uk

Abstract: It has been previously established that large networks of integrate-and-fire neurons with sparse, random connectivity can sustain irregular asynchronous activity [1][2][3][4]. This self-sustained asynchronous irregular (AI) activity facilitates rapid response to small changes in input and mimics activity patterns observed in cortical neurons [5][6]. For such patterns to emerge, appropriate adjustments of specific parameters are required to achieve AI activity in balanced networks with sparse random connectivity.

Keywords: Asynchronous Irregular Activity; Neuromorphic Hardware; real-time computing.

Introduction

Vogels and Abbott [5] systematically varied the strengths of the excitatory and inhibitory synapses of all neurons in the network to demonstrate it was possible to achieve AI state activity by meeting three conditions: sustained activity, relatively low firing rates, and ISI CVs near 1. They explored the impact of synaptic conductance on the stability, firing rate and irregularity of a balanced network in order to facilitate the propagation of signals. Their network consisted of 8000 excitatory and 2000 inhibitory conductance-based leaky integrate-and-fire neurons.

For robotic and biomedical applications of such spiking networks, real-time operation is required. Conventional computer systems are unable to achieve real-time simulation of spiking AI networks within practical limits of system size and power consumption. We thus employed specialised neuromorphic hardware, “SpiNNaker”, a multicore system that is optimised towards real-time simulations of large-scale spiking neural networks [7]. Its massively parallel architecture is inspired by computational principles found in the brain. The system we used allows us to simulate tens of thousands of spiking neurons in real-time. We leverage this computing power for a parameter search that finds configurations of synaptic conductance in which self-sustained asynchronous irregular activity is observed in the network.

Experimental

We ran simulations varying excitatory and inhibitory conductance within the parameter space established by Vogels and Abbott’s [5] parameter search. Each simulation consisted of 10,000 randomly connected conductance based (COBA) LIF neurons. It is typical to simulate Spiking Neural Networks with a timestep (dt) of <1ms. Using the SpiNNaker system for real-time simulation comes with a sacrifice in time resolution, with a minimum timestep of 1ms. This sacrifice can cause inaccuracies to accumulate over time which may result in different results from identical simulations at different time steps. Therefore, we also conducted the Vogels and Abbott [5] parameter search with a timestep of both 1ms and 0.1ms to analyse the dependency on timestep duration. Vogels and Abbott provided input spike trains generated by a Poisson process for 30ms at 180Hz. Due to hardware

limitations of the firing rate, we provided initial input to this network with Poisson process input spikes only at 100Hz over 50ms.

Results and discussion

Figure 1 shows a reproduction of the Vogels and Abbott [6] parameter search simulated on the SpiNNaker hardware with both a 0.1ms timestep (**a,b,c**) and 'real-time' simulation with a 1ms timestep (**d,e,f**). The metrics plotted are taken from the activity of 10% of both the excitatory and inhibitory populations. It is clear from these results the significant impact that timestep has on the network stability, firing rate and coefficient of variation of the simulated network. The 1ms timestep provides stability in removal of noise from the network activity, this allows the network to maintain and propagate the initial spiking input but also promotes synchronous activity within the network.

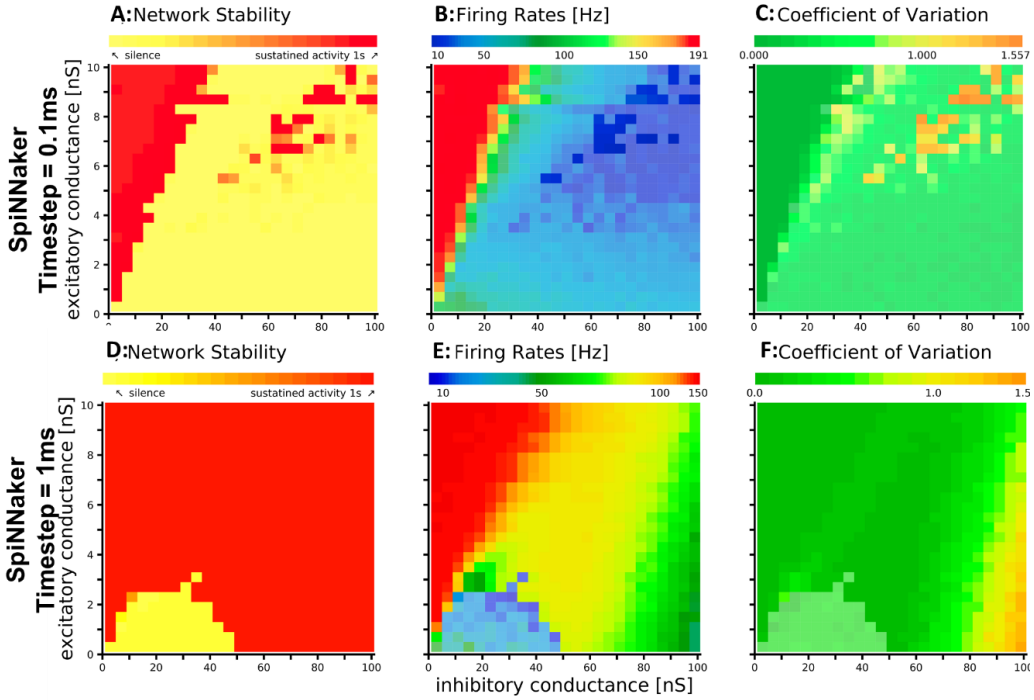

Figure 1. Results of Running Parameter Search on SpiNNaker Hardware at 0.1ms and 1ms timesteps. Network stability, Firing Rates in Hz and Coefficient of Variation calculated for pairs of synaptic excitatory and inhibitory conductance.

Conclusion

Hardware limitations introduced by the SpiNNaker hardware on simulating at a 0.1ms and 1ms timestep meant we had to reduce the maximum firing rate of the Poisson input. This hindered our ability to produce asynchronous irregular activity within even a large randomly connected conductance based LIF spiking neural network simulation. We therefore were only able to achieve AI activity within a select few simulations in the conductance parameter space with a 0.1ms timestep.

Reference list

[1] van Vreeswijk, C. & Sompolinsky, H. *Neural Computation* **10**, 1321-1371. (1998)
[2] Lerchner, A.; Ahmadi, M. & Hertz, J., *Neurocomputing* **58-60**, 935-940. (2004),
[3] Mehring, C.; Hehl, U.; Kubo, M.; Diesmann, M. & Aertsen, A., *Biological Cybernetics* **88**, 395-408. (2003)
[4] Brunel, N., *Journal of computational neuroscience* **8**, 183–208. (2000),
[5] Vogels, T. P. & Abbott, L. F., *Journal of neuroscience* **25**, 10786--10795. (2005)
[6] Vogels, T. P.; Sprekeler, H.; Zenke, F.; Clopath, C. & Gerstner, W. *Science* **334**, 1569–1573. (2011)
[7] Furber, S.B.; Galluppi, F.; Temple, S; Plana, L. A., *Proceedings of the IEEE* **102**, 652–665. (2014)

Graphene Aerogel deposition methods and its fabrication techniques as Energy storage devices

Himayasri Rao Lekkala[1], Dr Paul Sayers[2]
[1]University of Hertfordshire
[2]Bangor University

Graphene has rapidly achieved global recognition as an advanced engineering material due to its exclusive mechanical, optical, thermal and electrical properties. The context of the research is that the composite materials based on Graphene possess excellent potential for energy storage. To date, several fabrication techniques of these composite materials and their energy storage applications have been explored. The objective of the research presented here is to fabricate Supercapacitors based on Graphene Aerogels [GA] shown in figure (1.1). The physical properties of GA such as high surface area, porosity, electrical conductivity, specific capacitance and cyclic stabilities make it an excellent material for energy storage. Typically, GA can be employed between PMMA layers and metal electrodes like a double layer capacitor.

Here we report the manufacture of GA solutions using acetone, ethanol, isopropanol, methanol, water and PMMA as shown in the figure (1.2). The methodology involves drop casting these solutions between metal electrodes to fabricate an energy storage device demonstrating the characteristics of a hybrid supercapacitor, as shown in the figures (1.3) and (1.4). This study presents the fabrication, testing and comparison of the influence of different solvents on the energy storage characteristics of Graphene Aerogels.

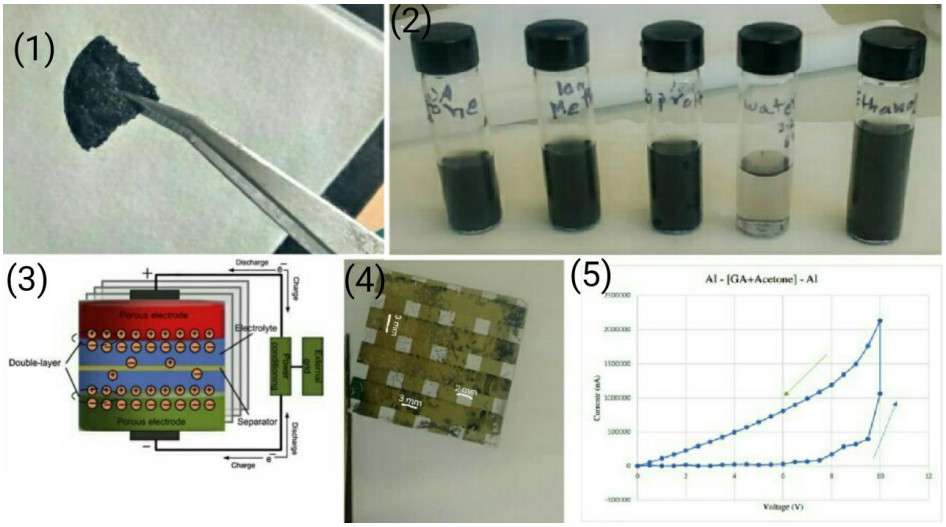

Figure 1 A small chunk of Graphene Aerogels [GA] pealed from bulk (2) GA solutions – Acetone+GA, Methanol+GA, Isopropanol+GA, Water+GA & Ethanol+GA [from left] (3) Schematic diagram of a Supercapacitor [2] (4) Fabricated

The V-I characteristics of all the fabricated devices were plotted. Results obtained using the Aluminium-[Acetone+GA]-Aluminium device are shown in figure (5) for reference. The thickness of each device was measured using a profilometer and the capacitance using an LCR meter. The maximum current produced was 0.01 A at 10 volts by a 3x3 mm and 1.3 um thick Al-[GA+PMMA 950+Acetone]-Al device with a capacitance value 22.17 µF. The value of current obtained is far better

than 1.6 Pico amps as produced by an Al-[PMMA+GA+PMMA]-Al device [1]. It can be concluded that this method worked well, generating significant improvements in the output characteristics of the fabricated storage devices.

References:-

[1] E. Cooke, "Investigating Graphene Aerogel and the Feasibility of its Application within Energy Storage Devices", Bangor University, 2017.
[2] X. Luo, J. Wang, M. Dooner and J. Clarke, "Overview of current development in electrical energy storage technologies and the application potential in power system operation", Applied Energy, vol. 137, pp. 511-536, 2015.

Modelling Adaptation through Social Allostasis: Modulating the Effects of Social Touch with Oxytocin in Embodied Agents

Imran Khan[1] and Lola Cañamero[1]

[1]Embodied Emotion, Cognition and (Inter-)Action Lab, School of Engineering and Computer Science, University of Hertfordshire, Hatfield AL10 9AB, UK

Social allostasis is a mechanism of adaptation that permits individuals to dynamically adapt their physiology to changing physical and social conditions. Oxytocin (OT) is widely considered to be one of the hormones that drives and adapts social behaviours. While its precise effects remain unclear, two areas where OT may promote adaptation are by affecting social salience and affecting internal responses of performing social behaviours. We present a model and experiments that investigate the effects and adaptive value of allostatic processes based on hormonal (OT) modulation of affective elements of a social behaviour. We study this through a simulated model (using the NetLogo platform) that adapts the intensity of physiological satisfaction of a social behaviour (social touch) as a function of dynamic internal OT levels. We also investigate its effects on the viability of the agent in a variety of food-related conditions that pose survival challenges.

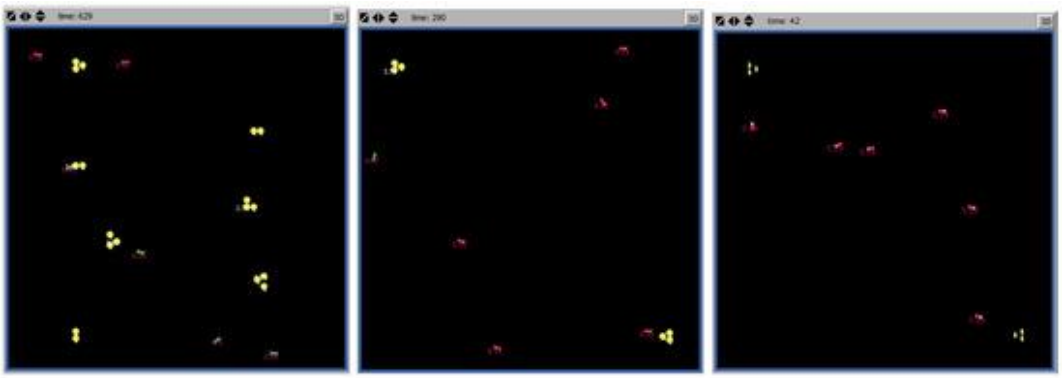

Figure 1: Visual representation of the three world conditions (Easy, Challenging and Super Challenging), each with different food availability. Agents are represented by bugs, and food resources are represented by yellow circles.

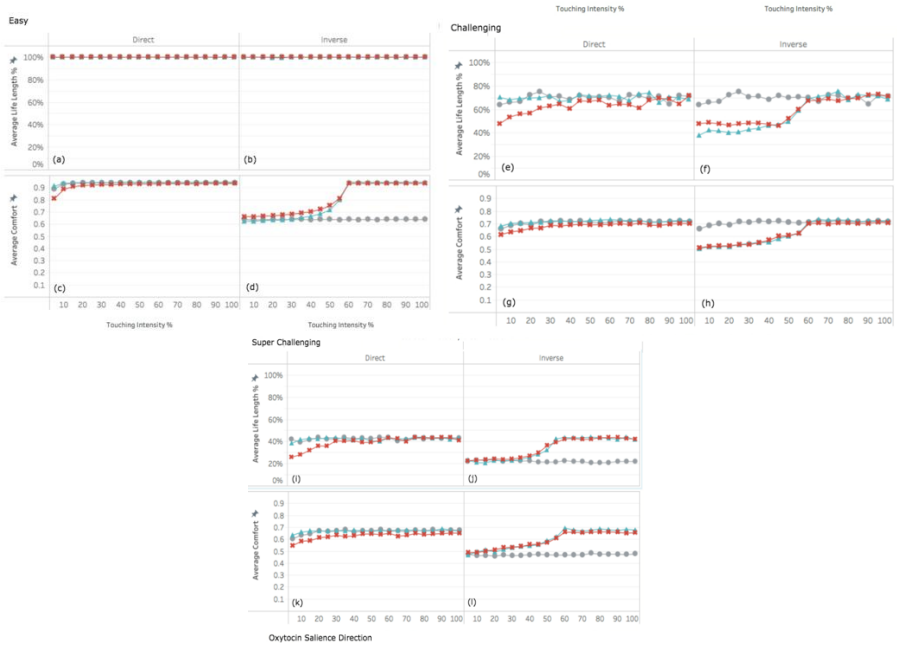

Figure 2: Aggregated results of simulation runs showing Average Life Length and Comfort Levels of agents across all three world conditions (Easy, Challenging and Super Challenging).

Our results show that the effects of these modulatory mechanisms have different (positive or negative) adaptive value across different groups and under different environmental circumstance in a way that supports the context-dependent nature of OT, put forward by the interactionist approach to OT modulation in biological agents. These results also support the hypothesis that there is no "one-size-fits-all" effect of the hormone, but that its effects should instead be adapted to an agent's "understanding" or perception of its internal and social environment. In terms of simulation models, this means that OT modulation of the mechanisms that we have described should be context-dependent in order to maximise viability of our socially adaptive agents, illustrating the relevance of social allostasis mechanisms.

Battery Energy Storage Systems in a Smart Electric Power Grid

Eheda Hassan[1*], Mouloud Denai[1], and Georgios Pissanidis[1]
[1]University of Hertfordshire, UK
*Corresponding Author: eheda222@hotmail.com

Keywords: smart grid; energy storage; renewable energy; electric grid; power grid.

Increasing the use of energy storages on the electric power grid allows growth of renewable energy generation sources to be implemented due to their compatibility in the system. As PV solar cells get charged up to peak capacity on a sunny afternoon and in some cases over-supplying the consumer demand, instead of the excess generation going to waste it can be used to charge up battery storage units available in the system which can be discharged in the evening when the sun has set and consumer demand risen up again. Remainder of the consumer demand can be taken from the electric grid as next priority [1].

Simulations are made through MATLAB and OpenDSS. IEEE and EPRI distribution circuits are used to imitate real energy networks and tested out with various scenarios to obtain desired results. This certain experiment focusses on gathering PV irradiance data with an implemented battery energy storage to follow the PV loadshape, smooth the peaks and troughs by charging and discharging the battery in order to provide a level flow of energy as well as peak shave in order to avoid damaging elements in the grid and avoid surplus energy [2]. See figure 1.

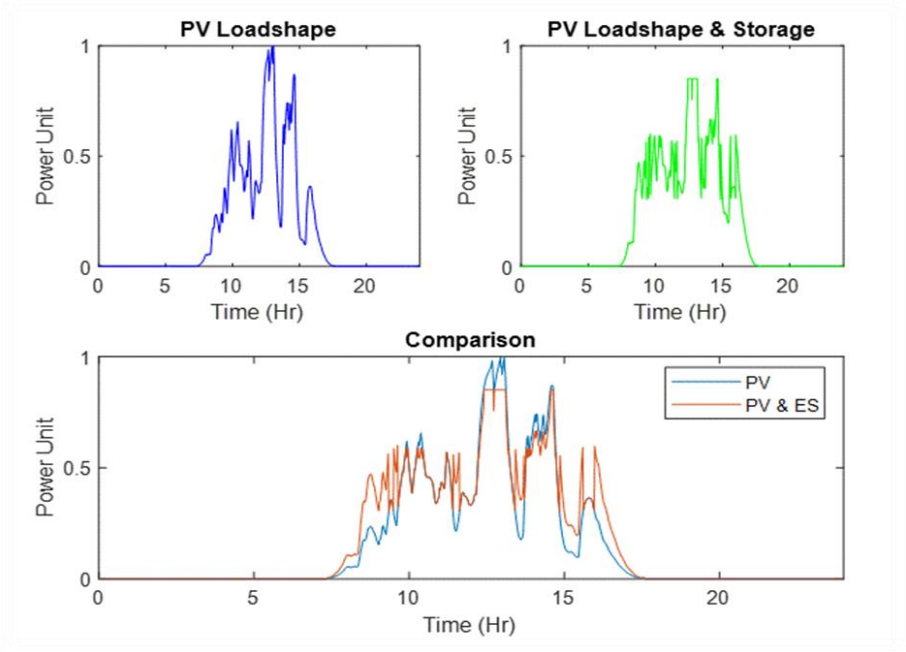

Figure 1: Top left plot is the PV solar irradiance, top right plot is the solar irradiance after energy storage contribution and the bottom plot shows the visual difference of the two on the same plot.

The overall result is to reduce element overloads on the grid as well as variable energy generation with charged-up energy storage units available. It eliminates high to low energy demand shifts and replaces reserves required for the system. This allows the grid to be more stable and reliable by

managing congestion and allowing operator flexibility by providing consumer demand with a constant supply of energy from the available resources and elements in the grid [3].

The more energy storage units available on the UK electric grid system, the more renewable energy sources can be implemented, the faster fossil-fire power plants can be shut down bringing the industry one step closer to a more economically friendly future.

Reference list

[1] G. Gruosso, P. Maffezzoni, Z. Zhang and L. Daniel. *Probabilistic Load Flow Methodology for Distribution Networks including Loads Uncertainty.* (2019). **International Journal of Electrical Power & Energy Systems.** V.106, p.392-400. https://doi.org/10.1016/j.ijepes.2018.10.023
[2] R. C. Dugan, J. A. Taylor and D. Montenegro. *Energy Storage Modeling for Distribution Planning.* (2016). **IEEE Transactions on Industry Applications.** V.53 p.954-962. https://doi.org/10.1109/repc.2016.11
[3] G. Hilton, A. Cruden and J. Kent. *Comparative Analysis of Domestic and Feeder Connected Batteries for Low Voltage Networks with High Photovoltaic Penetration.* (2017). **Journal of Energy Storage, Elsevier.** V.13, p.334-343. https://doi.org/10.1016/j.est.2017.07.019

Computational modelling of short-term depression at a cerebellar synapse in health and disease

Julia Goncharenko*, Neil Davey, Maria Schilstra and Volker Steuber

Centre for Computer Science and Informatics Research, University of Hertfordshire, Hatfield, AL10 9AB, UK
*corresponding author: i.goncharenko@herts.ac.uk

The aim of this study is to investigate the mechanism of action of 4-aminopyridine (4-AP), a non-selective potassium channel blocker, in the treatment of downbeat nystagmus (DBN), which is a common eye fixation disorder.

Keywords: short-term depression; cerebellum; nystagmus; computational modelling; 4-aminopyridine.

DBN has been linked to pathological activity of neurons in the cerebellum, in particular, an increased activity of floccular target neurons (FTNs) in the vestibular nuclei. Previously, this increase in FTN activity in DBN has been explained by a pathological decrease in the activity of inhibitory Purkinje cell inputs to FTNs. The therapeutic action of 4-AP could then be explained by an increase in Purkinje cell spiking by the potassium channel blocker, which could in turn decrease the unphysiologically high FTN spike rate and thus cure DBN [1]. However, electrophysiological recordings of Purkinje cells in cerebellar slices from tottering (tg/tg) mice, a commonly used model system of DBN, have recently shown that the consequence of applications of therapeutic concentrations of 4-AP is in fact an increase in the regularity of Purkinje cell spiking, which is disturbed in tg/tg mice [2]. In these experiments, no increase in the Purkinje cell activity by 4-AP was found.

To investigate the influence of changes in the regularity of Purkinje cell spiking on the activity of FTNs, Glasauer and colleagues performed a series of computer simulations using a simple conductance based model of an FTN [3]. They found that changes in the regularity of the Purkinje cell activity affected the FTN spike rate only when the Purkinje cell input to the FTN model was synchronised. Furthermore, their simulations predicted that the effect of an increased irregularity of the synchronised Purkinje cell input to the FTN was a decreased activity in the FTN model, due to the more frequent occurrence of smaller inter-spike intervals in the irregular inhibitory Purkinje cell input. Thus, these simulation results are unable to explain the link between the increased irregularity of Purkinje cell activity and the increased FTN spike rate during DBN, and they also cannot explain the beneficial effect of 4-AP.

Here we suggest that the explanation for the apparent contradiction between the experimental [2] and computational [3] results is that Glasauer and colleagues did not include short-term depression (STD) at the synapses between Purkinje cells and FTNs in their simulations. To simulate the effect of irregular versus regular Purkinje cell input we used a conductance based morphologically realistic model of a cerebellar nucleus (CN) neuron [4, 5] as an FTN model, and we included STD at the inhibitory Purkinje cell synapses to the model [5]. In our simulations, the coefficients of variation of the irregular and regular Purkinje cell spike trains during DBN and after 4-AP treatment, respectively, were taken from electrophysiological data from wild-type and tg/tg mice [6].

For both synchronised and unsynchronised Purkinje cell input to the FTN model, we found that irregular (DBN) input spike trains resulted in higher FTN spike rates than regular (4-AP) ones. In the

presence of unsynchronised Purkinje cell input, the increase of the FTN spike rate during simulated DBN and the corresponding decrease for simulated 4-AP treatment depended on STD at the Purkinje cell synapses. Our results provide a potential explanation for the underlying mechanism of DBN and its treatment with 4-AP.

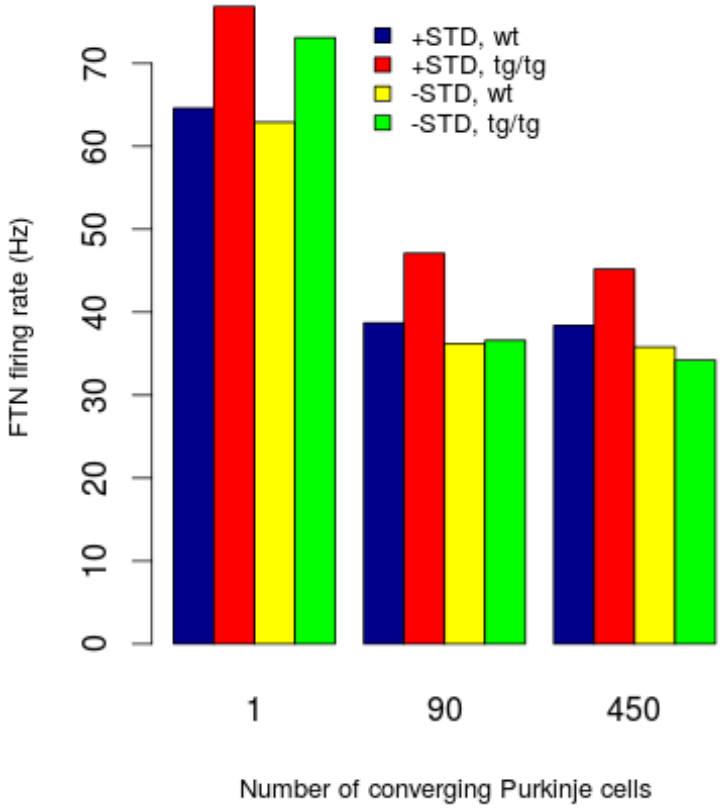

Figure 1. Irregular Purkinje cell input results in increased spike output of the FTN model.

We used a compartmental conductance based model of a CN neuron [4, 5] as a model of a flocculus target neuron (FTN), given the indistinguishable physiology of both neuron types. The FTN model was presented with regular and irregular Purkinje cell input at 60 Hz with coefficients of variation (CV) of 0.34 and 0.66, respectively. These CVs values were based on experimental data from wild-type (wt) and tottering (tg/tg) mice, which are commonly used as a model system for DBN (and represented, in our case, also the effect of 4-AP treatment of DBN). Simulations were performed in the presence and absence of STD at the Purkinje cell – FTN synapses, and for different numbers of Purkinje cells converging onto the FTN model. Convergence ratios can also be interpreted as synchronicity of Purkinje cell inputs, with a convergence ratio of 1 indicating fully synchronised Purkinje cell input to the FTN. The results show that for a convergence ratio of 1 (or fully synchronised Purkinje cell input), irregular Purkinje cell input led to an increase in the FTN spike rate of 16% compared to regular input in the presence of STD, and to a 14% increase in the absence of STD. For higher convergence ratios of 90 and 450 (or desynchronised Purkinje cell input), an input irregularity based FTN spike rate increase only occurred in the presence of STD, with increases of 18% and 15% for convergence ratios of 90 and 450, respectively.

Reference list

[1] A1. Glasauer S, Kalla R, Buttner U, Strupp M, Brandt T: 4-aminopyridine restores visual ocular motor function in upbeat nystagmus. J Neurol Neurosurg. Psychiatry 2005, 76:451– 453.

[2] Alvina K, Khodakhah K: The therapeutic mode of action of 4-aminopyridine in cerebellar ataxia. J. Neurosci. 2010, 30: 7258–7268.
[3] Glasauer S, Rössert C and Strupp M: The role of regularity and synchrony of cerebellar Purkinje cells for pathological nystagmus. Ann. N. Y. Acad. Sci. 2011, 1233:162-167.
[4] Steuber V, Schultheiss NV, Silver RA, de Schutter E, Jaeger D: Determinants of synaptic integration and heterogeniety in rebound firing explored with data-driven models of deep cerebellar nucleus cells. J. Comp. Neurosci. 2011, 30:633-658.
[5] Luthman J, Hoebeek FE, Maex R, Davey N, Adams R, de Zeeuw CI, Steuber V: STD-dependent and independent encoding of input irregularity as spike rate in a computational model of cerebellar nucleus neuron. Cerebellum 2011, 10:667-682.
[6] Hoebeek FE, Stahl JS, van Alphen AM, Schonewille M, Luo C, Rutteman M, van den Maagdenberg AM, Molenaar PC, Goossens HH, Frens MA et al: Increased noise level of Purkinje cell activities minimizes impact of their modulation during sensorimotor control. Neuron 2005, 45(6):953–965.

Validation of a DNA library preparation model using a genetic algorithm

Nathan Beka[1*], Rene te Boerkhorst[1], and Rod Adams[1], and Neil Davey[1]
[1]*University of Hertfordshire*
*n.beka@herts.ac.uk

Our research is a study of artefacts associated with the library preparation stage of DNA sequencing and how they may be overcome to improve final sequencing outcomes. To investigate these issues a library preparation model was developed, and its associated issues were implemented in the model. To validate our model a genetic algorithm (GA) is used to find optimal parameters for our library preparation model. Our final results show that using parameters selected by the GA we were able to acceptably mimic real-world coverage.

Keywords: Next Generation Sequencing; Library Preparation; Genetic Algorithm; DNA; Coverage

Introduction

Next-generation sequencing has empowered genomics by making it possible to sequence genomes at a lower cost and less time compared to the traditional Sanger method [1]. However, these improvements suffer from reduced accuracy when compared with the Sanger method. During the library preparation stage of sequencing, artefacts can be introduced that affect the reliability of a read [2]. These artefacts can arise from biases due to the structure of the genome, such as preferential splitting of DNA between specific nucleotides [3], bias of adapter ligation towards certain base pair identities [4], and temperature dependent denaturation due to nucleotide composition [5].

Experimental

To investigate this a library preparation model was developed to simulate the occurrences and effects of such artefacts. Our model simulates the following steps of the library preparation process: i) DNA fragmentation, ii) adapter ligation and iii) PCR amplification. To do this a set of parameters characterizing these three steps and a DNA sequence are fed as input to the model and the expected output is coverage scores across the genome. In order to find optimal parameters that would lead to coverage values comparable to those found in real-world sequencing a Genetic Algorithm (GA) was applied. As a fitness function we used the correlation between an actually sequenced genome and the coverage from subjecting that genome to the model.

Results and discussion

After running the GA, we were able to acquire parameters which delivered coverage results that matched the actual coverage for 2 genomes. The first was a 50kbp (kilo base pairs) section of the *Mycobacterium tuberculosis* strain H37Rv genome where the fitness score was 0.83 (Figure 1a). In the second a 50kbp section of the *Plasmodium falciparum* strain 3D7 genome where the fitness score was 0.86 (Figure 1b). In both cases the acquired parameters were able to acceptably mimic coverage. Following these results, we decided to test the acquired parameters on contiguous sections of the tested genomes. In the case of the *tuberculosis* genome it was not possible to mimic coverage across the genome (Figure 2a), but with plasmodium the parameters were able to mimic coverage (Figure 2b). This led us to believe that mimicking coverage across a genome was dependent on its structure.

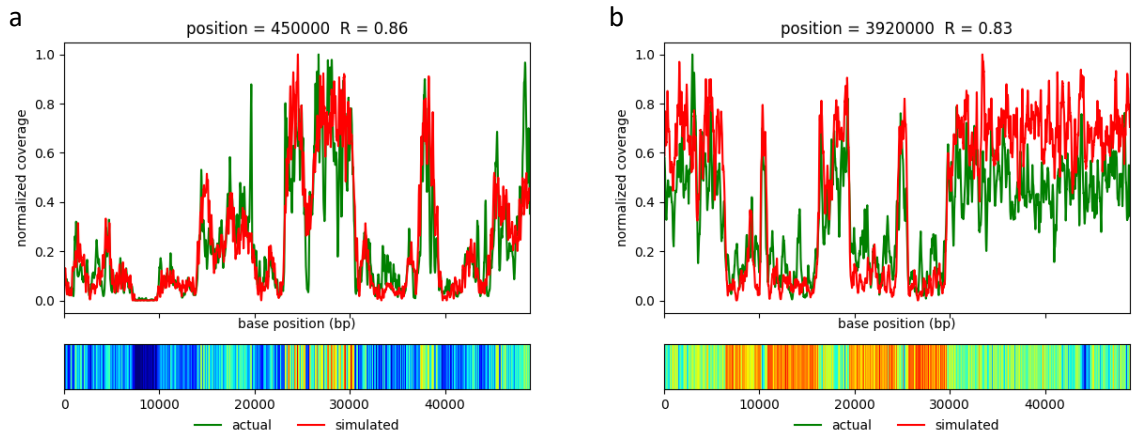

Figure 1. Comparison of results for simulated sequencing and actual sequencing run after evolving model parameters. The colour bar shows levels of base composition bias (blue - red = increasing GC content). (A) Results for section of Mycobacterium tuberculosis genome. (B) Results for section of Plasmodium falciparum genome.

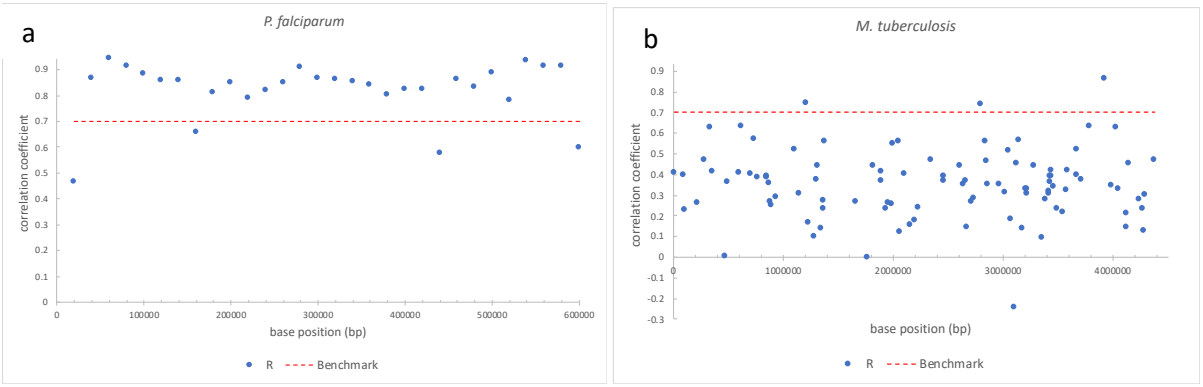

Figure 2. Parameters with the highest fitness score taken from a section of the genome are tested on other parts of the genome. (A) The parameters could not reliably mimic coverage across the Mycobacterium tuberculosis genome. (B) For the Plasmodium falciparum genome, the parameters were able to mimic coverage across the genome.

Conclusion

These results confirm that a GA can be used to optimize our model to obtain coverage values similar to those obtained in real-world sequencing runs. However, in how far the parameters acquired by the GA are representative across a genome depends on the species-specific structure of that genome Our next objective is to analyze the effect of combined and possible knock-on effects of chosen parameter values on coverage given the nucleotide composition of an input genome.

References

[1] E. L. van Dijk, Y. Jaszczyszyn, and C. Thermes, “Library preparation methods for next-generation sequencing: Tone down the bias,” Experimental Cell Research, vol. 322, no. 1, pp. 12–20, Mar. 2014.
[2] M. G. Ross et al., “Characterizing and measuring bias in sequence data,” Genome Biology, vol. 14, no. 5, p. R51, May 2013.
[3] M. S. Poptsova et al., “Non-random DNA fragmentation in next-generation sequencing.,” Scientific reports, vol. 4, p. 4532, Jan. 2014.
[4] A. Seguin-Orlando et al., “Ligation bias in illumina next-generation DNA libraries: implications for sequencing ancient genomes.,” PloS one, vol. 8, no. 10, p. e78575, Jan. 2013.
[5] D. Aird et al., “Analyzing and minimizing PCR amplification bias in Illumina sequencing libraries.,” Genome biology, vol. 12, no. 2, p. R18, Jan. 2011.

Computational Dynamics of Biochemical Systems

Ágnes Bonivárt, Chrystopher Nehaniv, Shabnam Kadir

University of Hertfordshire

a.bonivart@herts.ac.uk

Introduction

Biochemical systems can be large and complex, and therefore difficult to study, and their properties and dynamics are difficult to compute [1]. We address this problem in our research by developing methods for building them up from simpler systems which are easier to analyse and understand. We also relate models of biochemical systems that use different formalisms (e.g. Petri-nets, differential equation systems, Metabolic Control Analysis) by formulating them as categories and mapping them on each other in order to gain a new understanding about one domain based on knowledge about another very different domain. We define functors, i.e. structure preserving maps between the different categories.

A major challenge in Systems Biology is to determine the relationship between structure and function in complex biochemical networks. The underlying kinetics is usually unknown, so a structural approach is needed [2]. One such approach is to investigate the stoichiometry matrix of the biochemical reaction system. For example, we can examine under what conditions metabolic networks operate at steady state. Even if the system is not in steady state we can obtain conservation relations among the chemical species that are constant on all trajectories. Both steady state fluxes and conservation relations are investigated by the null-spaces of the stoichiometry matrix [3, 4]. It has been found that all admissible flux vectors which could correspond to steady state of the biochemical network form a convex polyhedral cone [5]. Though the study of metabolic networks by means of their steady state stoichiometry is a well established research field, there are still open questions, in particular the relationship between dynamics of the subsystems and the dynamics of the whole system.

Another approach we have recently started is to compute the minors of the stoichiometry matrix, which are the so called Plücker coordinates of a Grassmannian variety. Each k x k minor can be thought of as the flux in the k species due to a particular subset of k reactions. We are examining what these coordinates mean in terms of the dynamics of the biochemical system. We are currently investigating what happens to the Plücker coordinates when we combine subsystems as co-product and push-outs.

Results

We have managed to formulate categories of the different models of biochemical systems, like BioChem [6], MCA and ODE, and to define functors between them. We have also defined morphisms between objects in BioChem and MCA. We have results on how the flux vectors change when gluing systems category theoretically. We have also proven theorems on isomorphisms of biochemical systems.

$S_1 + Y_1 \rightarrow 2X_1$ $\quad$ $S_2 + Y_2 \rightarrow 2X_2$

$2X_1 \rightarrow X_1 + Y_1$ $\quad$ $2X_2 \rightarrow X_2 + Y_2$

$X_1 + Y_1 \rightarrow Y_1 + P_1$ $\quad$ $X_2 + Y_2 \rightarrow Y_2 + P_2$

$X_1 \rightarrow P_1$ $\quad$ $X_2 \rightarrow P_2$

Figure 1: Coproduct of a Biochemical System

Conclusion

In spite of the immense effort made by scientists to study complex biochemical systems there still is a need for finding methods by which we can build the whole system up from its subsystems. Applying category theoretical approach is a new and promising idea.

References:

1. R. Urbanczik, C. Wagner. An Improved Algorithm for Stoichiometric Network Anal-ysis: Theory and Applications, Bioinformatics, 21: 1203-1210, 2004.
2. Christine Reder. Metabolic Control Theory: A Structural Approach, Journal of Theoretical Biology, 135:175–201, 1988.
3. S. Schuster, C. Hilgetag, J.H Woods, D.A Fell. Elementary Modes of Functioning in Biochemical Networks, Worldscientific
4. R. Urbanczik, C. Wagner. An Improved Algorithm for Stoichiometric Network Anal- ysis: Theory and Applications, Bioinformatics, 21: 1203-1210, 2004.
5. Clemens Wagner, Robert Urbanczik. The Geometry of the Flux Cone of a Metabolic Network Biophysical Journal, 89: 3837-3845, 2005
6. Chrystopher L. Nehaniv, Fariba Karimi, Daniel Schreckling, Nicoline den Breems, Ágnes Bonivárt, Maria J. Schilstra, Alastair J. Munro. Functors and Adjoints for Dis- crete and Continuous Dynamical Cellular Systems Symmetries BIOMICS Deliverable D2.1, 2014.

The Correlation between EEG Signals Varying with Distance for Datasets With and Without Medical Condition

Ronakben Bhavsar[1*], Yi Sun[1], Na Helian[1], Neil Davey[1], David Mayor[1] and Tony Steffert[2]
[1]University of Hertfordshire
[2]The Open University
*r.bhavsar2@herts.ac.uk

Electroencephalogram (EEG) are time varying signal, and give different signals at the different position of electrodes. There might be a correlation between a pair of these signals; more likely related to the actual positions of electrodes. In this paper, we show that the correlation is related to the physical distance between electrodes as measured on the scalp for datasets without medical condition, but might not for datasets with medical conditions. This finding is independent of participants and brain hemisphere. Our results indicate that the EEG signal is not transmitted via neurons but through white matter in a brain.

Keywords: EEG; Independent Component Analysis (ICA); Cross-correlation; Time Series Data; Biomedical Data.

Introduction

An Electroencephalogram (EEG) is a time varying signal, and the electrodes at different positions give different time varying signals. Our previous work indicated that there was a correlation between these signals [1]. However, that research only focused on datasets without any medical conditions. In this work, we analyse datasets not only without medical conditions, but also with medical conditions, such as Epilepsy, Autism, and Seizure.

Dataset Information

This research utilised six datasets including; 3 (Dataset 1, Dataset 2, and Dataset 3) without medical condition [2], and 3 (Dataset 4, Dataset 5, and Dataset 6) with medical condition [3] [4], as shown in Table 1.

Labels	Dataset 1	Dataset 2	Dataset 3	Dataset 4	Dataset 5	Dataset 6
Medical Condition	None	None	None	Epilepsy	Autism	Seizure
Participants	16	20	32	5	13	12
Electrodes	19	10	15	19	19	19
Paired Electrodes	171 Pairs	45 Pairs	105 Pairs	171 Pairs	171 Pairs	171 Pairs

Table 1. Datasets Information

Experiments and Results

The EEG signals were processed to remove artefacts, such as eye blinks, eye movements, jaw movements and muscle movements, by using Independent Component Analysis (ICA). In order to obtain distance in centimetres (cm) between electrodes, a measuring tape was used to measure distance using a straight line distance between two electrodes on a cap - not the distance as measured over the surface (curved line) of the scalp. Cross-correlation has been calculated on the processed EEG signals. Figure 1 shows the average correlation results of participants for electrode Fp1 on analysing all six datasets, where electrode Fp1 has been chosen randomly across all 19 electrodes for all datasets to show the Cross-correlation performance - other electrodes have similar results. Figure 1 **(A), (B)**,

(C), and **(E)** demonstrates that there is an inverse linear relationship between Cross-correlation value and distance. Whereas Figure 1 **(D),** and **(F)** do not indicate any linear dependency.

Discussion and Conclusion

One of the main conclusions of this work is that electrical activity correlates linearly with straight line physical distance (that is when the distance increases the correlation decreases) for participants without medical conditions. However, participants with medical conditions such as Epilepsy and Seizure, the linear dependency might not exist. We lack of the expertise to provide possible reasons for this, but think this might be of interest to the people working in medical area. The second conclusion from this work is that the correlation is independent of brain hemisphere for all datasets. This suggests that most probably the electrical signals are transmitted through the white matter of the brain [3]. We assume that signal transmission is through white matter because of the commissural tracts within the white matter which connect the two hemispheres of the brain. This means, in practice it does not matter which side of the median plane you place the electrodes.

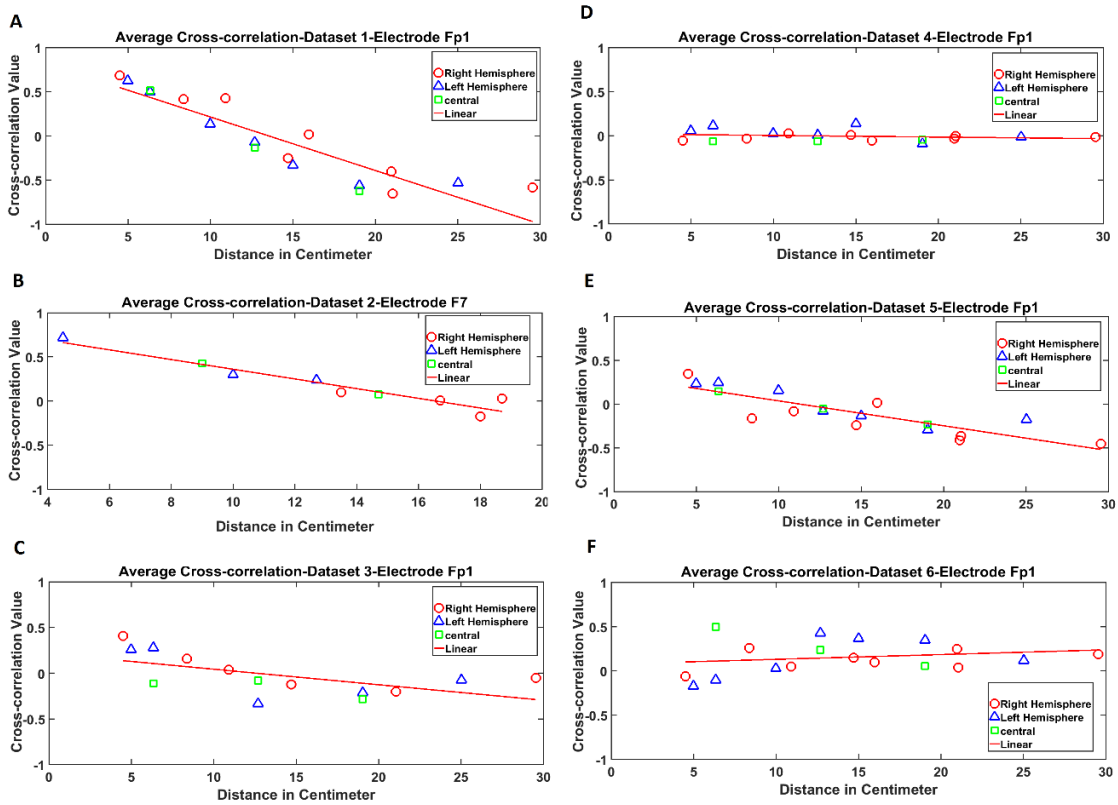

Figure 1. Cross-correlation between electrodes at varying distance on all datasets. Where, ***(A)*** *Dataset 1,* ***(B)*** *Dataset 2,* ***(C)*** *Dataset 3, are without any medical condition, and* ***(D)*** *Dataset 6,* ***(E)*** *Dataset 7, and* ***(F)*** *Dataset 8, are with medical condition Autism, Epilepsy, and Epileptic Seizures, respectively.*

References

[1] Bhavsar, R., Sun, Y., Helian, N., Davey, N., Mayor, D. and Steffert, T., "The Correlation between EEG Signals as Measured in Different Positions on Scalp Varying with Distance.," Procedia Computer Science., vol. 123, pp. 92-97, 2018.
[2] Koelstra, "Deap: A database for emotion analysis; using physiological signals," in IEEE Transactions on Affective Computing, 2012.
[3] Fields, R.D., 2008., "White matter matters.," Scientific American, vol. 293, no. 3, pp. 54-61, 2008.
[4] D. D. a. E. K. Taniskidou, "UCI machine learning repository," 2017. [Online]. Available: http://epileptologie-bonn.de/cms/upload/workgroup/lehnertz/eegdata.html. [Accessed 2018].
[5] A. L. Goldberger, "Component of a new research resource for complex physiologic signals.," 2000. [Online]. Available: https://physionet.org/pn6/chbmit/. [Accessed 2018].